There are reports that evaluating fraction of joints by ultrasonography is a good way to predict future joint damage [11–12]. One study reported that 5 of the 28 joints with MTP2 and MTP5 joints, namely, wrist, MCP2, MCP3, PIP2, and PIP3 joints, are enough for ultrasonography evaluation [12]. Their data seems to be consistent with our results as they selected at least two joints from three different groups into which the 28-joint symptoms were classified. As ultrasonography usually surpasses physical examination in terms of the sensitivity to detect synovitis, it is interesting to analyze whether the assessments of synovitis using ultrasonography show the same pattern of synovitis over the 28 joints in RA.

Our results indicate that RA does not develop synovitis in the 28 joints with the same frequency and that the affected rate of each joint greatly varies from joint to joint. These different distributions of joint synovitis would lead to different distribution of joint destruction. Based on our results, the 28 joints can be categorized into three groups, and it is possible that some fractions of the 28 joints are less informative to assess disease activity than others. It would be interesting to develop a novel simplified joint core set, and analyze the correlation between joint damage and activity score based on this. It would be also interesting to characterize each of RA subsets in more detail.

Materials and Methods

Ethics Statement

Written informed consent to enroll in the database described below was obtained from most of the patients, but for some patients the information regarding the construction of this database was disclosed instead of obtaining written informed consent. Participants who were informed regarding the construction of the database (instead of obtaining written informed consent) were allowed to withdraw from the study if desired.

All data were de-identified and analyzed anonymously. This study was designed in accordance with the Helsinki Declaration. This study including the consent procedure was approved by the ethics committee of Kyoto University Graduate School and Faculty of Medicine.

The KURAMA database

The KURAMA (Kyoto University Rheumatoid Arthritis Management Alliance) database was established in 2011 at Kyoto University to store detailed clinical information and specimens from patients with arthritis and arthropathy. The alliance is composed of rheumatic disease-associated departments in Kyoto University Hospital as well as its allied, integrating previous database and specimen collections in each department and allied. A template for electronic clinical charts developed at Kyoto University Hospital in 2004 to evaluate joint involvements in RA patients was used to obtain joint assessments. Rheumatologists evaluated swelling and tenderness of the 28 joints in patients with RA on each visit and filled in the template. The synovitis information of the 28 joints and data for C-reactive protein and erythrocyte sedimentation rate were extracted from electronic clinical charts [15] and stored in the KURAMA database.

Patients and data of joint assessment

A total of 17,311 joint assessments from 1,314 patients with RA from 2005 to 2011 were obtained in a retrospective manner from the KURAMA database. All of the patients fulfilled ACR revised criteria for RA in 1987 [10] or ACR and EULAR classification criteria for RA in 2010 [16–17].

Analysis of affected frequencies in the 28 joints

RA patients were subdivided depending on whether their data were available in 2011 or not, and the affected frequency in each of the 28 joints was calculated. We compared the order of the affected frequency in the 28 joints between the two patient sets with Spearman's rank-sum coefficient. We separately analyzed the affected rates of joints for swelling and tenderness. When multiple joint assessments in different visits were available in the same patient with RA, we randomly selected one of the assessments as representative in the patient. We compared frequencies between tenderness and swellings for the 28 joints with Spearman's rank-sum coefficient.

Clustering of patients with RA

Clustering analyses were performed by Ward method, using randomly-selected 5,383 evaluations of the 28 joints from 1,314 patients with RA. These evaluations did not contain more than six assessments from each patient to avoid excess influence of particular patients. Affected rates were calculated for the three groups of joints (namely PIP joints, MCP joints and large and wrist joints) in this clustering analysis. For example, when a patient showed tenderness and swelling for all PIP joints, the affected rate of PIP joints in the patient is 2. When a patient showed tenderness for four MCP joints, the affected rate of MCP joints is 0.4.

RA patients were regarded as belonging to a particular group when more than 60% of evaluations belonging to the same patients with four or five evaluations were classified into the same group.

Analysis between RA subgroups and joint destruction

Joint destruction of hand joints in 246 patients with RA was evaluated by modified Sharp score by a trained rheumatologist who was not informed of the patients' characteristics (KM). Joint destruction rates were defined for the three groups of joints as a sum of scores divided by the full score in the joints group. For example, when a patient shows 50 as a sum of scores in the large and wrist group, the patient's joint destruction rate for the group is 0.463 (50/108).

Correlation of the 28 joints and statistical analysis

Correlations of joint symptoms among the 28 joints were estimated separately for tenderness and swelling. We randomly obtained one assessment of the 28 joints in each patient as a representative of the patient's joint assessments for maximization of the power. Kappa coefficient was used to analyze coincidence of joint symptoms in each pair of the 28 joints. Eigen vectors obtained in principal component analysis were used to analyze the deviation of joint symptoms. We resampled joint assessments for each patient and created four other sets of joint assessments. The same correlation analyses were performed using the four resampled assessments to confirm the correlation shown in the first assessment set. Right dominance of the synovitis and joint destruction was analyzed by binomial test. Dominant destruction of joints was evaluated by paired-t test. Statistical analysis was performed by R software or SPSS (ver18).

Supporting Information

Figure S1 Distribution of joint evaluation counts and patients across different years. A) Distribution of number of RA patients according to numbers of 28-joint assessments. B) Distribution of number of patients with RA whose joint assessment data were available from 2005 to 2011 in the KURAMA database. (TIF)

Figure S2 Good correlations between joint involvement rates in different sets of RA patients. Rates of joint involvement for A) swelling and B) tenderness were compared between the two different sets of RA patients. X and Y axes represent rates in the first set of RA patients in 2011 and those in the second set in 2005 to 2010, respectively.
(TIF)

Figure S3 Three groups of joints regardless of different sets of RA patients. Analysis using one of four resampled assessments in one of the two sets of RA patients is shown as a representative. The 1st and 2nd components of eigen vectors of the joint symptoms are plotted, using principal component analysis of the 28 joint involvement for tenderness (A) and swelling (C) or using that of the 20 joint involvement other than large and wrist joints for tenderness (B) and swelling (D). Green: large and wrist joints. Red: MCP joints. Blue: PIP joints.
(TIF)

Figure S4 Three groups of joints regardless of different evaluators. Analysis using one of five resampled assessments by one of the two groups of medical doctors is shown as a representative. The 1st and 2nd components of eigen vectors of the joint symptoms are plotted, using principal component analysis of the 28 joint involvement for tenderness (A) and swelling (C) or using that of the 20 joint involvement other than large and wrist joints for tenderness (B) and swelling (D). Green: large and wrist joints. Red: MCP joints. Blue: PIP joints.
(TIF)

Figure S5 Dominant destruction of large and wrist joints in the sixth subgroup of patients with RA. Box plots indicating the joint destruction rates in the three joint groups in subjects belonging to the sixth subgroup.
(TIF)

Figure S6 Destruction of large and wrist joints among the six subgroups of RA. Differences in destruction rates were plotted for each subject in the six subgroups. The difference was defined as: A) destruction rate of group of large and wrist joints – destruction rate of MCP joints and B) destruction rate of group of large and wrist joints – destruction rate of PIP joints.
(TIF)

Table S1 Rate of joint involvement for 28 joints in RA.
(DOC)

Table S2 Right-dominant joint destruction in RA. Patients who showed unilateral higher or lower scores in each element were analyzed.
(DOC)

Table S3 Mean affected rates of the three joint groups in the six subgroups of patients with RA.
(DOC)

Acknowledgments

We would like to thank to Mr. Wataru Yamamoto at Kurashiki Kosai Hospital for his excellent support to establish and maintain the KURAMA database. We also thank Drs Hisashi Yamanaka, Katsunori Ikari, and Ayako Nakajima at Institute of Rheumatology, Tokyo Women's Medical University for their kind instruction and advice for management of rheumatic diseases database.

Author Contributions

Evaluation of joint X-rays: KM. Conceived and designed the experiments: CT MH KO RY FM HI TF TM. Analyzed the data: CT. Contributed reagents/materials/analysis tools: CT MH KO RN KM N. Yamakawa H. Yoshifuji N. Yukawa DK TU H. Yoshitomi MF HI TF TM KY. Wrote the paper: CT.

References

1. Firestein GS (2003) Evolving concepts of rheumatoid arthritis. Nature 423: 356–361.
2. Drossaers-Bakker KW, de Buck M, van Zeben D, Zwinderman AH, Breedveld FC, et al. (1999) Long-term course and outcome of functional capacity in rheumatoid arthritis: the effect of disease activity and radiologic damage over time. Arthritis and Rheumatism 42: 1854–1860.
3. Smolen JS, Van Der Heijde DM, St Clair EW, Emery P, Bathon JM, et al. (2006) Predictors of joint damage in patients with early rheumatoid arthritis treated with high-dose methotrexate with or without concomitant infliximab: results from the ASPIRE trial. Arthritis and Rheumatism 54: 702–710.
4. Felson DT, Anderson JJ, Boers M, Bombardier C, Chernoff M, et al. (1993) The American College of Rheumatology preliminary core set of disease activity measures for rheumatoid arthritis clinical trials. The Committee on Outcome Measures in Rheumatoid Arthritis Clinical Trials. Arthritis and Rheumatism 36: 729–740.
5. van der Heijde DM, van 't Hof MA, van Riel PL, Theunisse LA, Lubberts EW, et al. (1990) Judging disease activity in clinical practice in rheumatoid arthritis: first step in the development of a disease activity score. Annals of the Rheumatic Diseases 49: 916–920.
6. van der Heijde DM, van't Hof MA, van Riel PL, van Leeuwen MA, van Rijswijk MH, et al. (1992) Validity of single variables and composite indices for measuring disease activity in rheumatoid arthritis. Annals of the Rheumatic Diseases 51: 177–181.
7. Smolen JS, Breedveld FC, Schiff MH, Kalden JR, Emery P, et al. (2003) A simplified disease activity index for rheumatoid arthritis for use in clinical practice. Rheumatology 42: 244–257.
8. Aletaha D, Smolen JS (2007) The Simplified Disease Activity Index (SDAI) and Clinical Disease Activity Index (CDAI) to monitor patients in standard clinical care. Best Pract Res Clin Rheumatol 21: 663–675.
9. Salaffi F, Cimmino MA, Leardini G, Gasparini S, Grassi W (2009) Disease activity assessment of rheumatoid arthritis in daily practice: validity, internal consistency, reliability and congruency of the Disease Activity Score including 28 joints (DAS28) compared with the Clinical Disease Activity Index (CDAI). Clinical and Experimental Rheumatology 27: 552–559.
10. Arnett FC, Edworthy SM, Bloch DA, McShane DJ, Fries JF, et al. (1988) The American Rheumatism Association 1987 revised criteria for the classification of rheumatoid arthritis. Arthritis Rheum 31: 315–324.
11. Scheel AK, Hermann KG, Kahler E, Pasewaldt D, Fritz J, et al. (2005) A novel ultrasonographic synovitis scoring system suitable for analyzing finger joint inflammation in rheumatoid arthritis. Arthritis and Rheumatism 52: 733–743.
12. Backhaus M, Ohrndorf S, Kellner H, Strunk J, Backhaus TM, et al. (2009) Evaluation of a novel 7-joint ultrasound score in daily rheumatologic practice: a pilot project. Arthritis and Rheumatism 61: 1194–1201.
13. van der Heijde D (2000) How to read radiographs according to the Sharp/van der Heijde method. Journal of Rheumatology 27: 261–263.
14. Machold KP, Stamm TA, Eberl GJ, Nell VK, Dunky A, et al. (2002) Very recent onset arthritis – clinical, laboratory, and radiological findings during the first year of disease. Journal of Rheumatology 29: 2278–2287.
15. Yamamoto K, Yamanaka K, Hatano E, Sumi E, Ishii T, et al. (2012) An eClinical trial system for cancer that integrates with clinical pathways and electronic medical records. Clin Trials 9: 408–417.
16. Aletaha D, Neogi T, Silman AJ, Funovits J, Felson DT, et al. (2010) 2010 Rheumatoid arthritis classification criteria: an American College of Rheumatology/European League Against Rheumatism collaborative initiative. Arthritis and Rheumatism 62: 2569–2581.
17. Aletaha D, Neogi T, Silman AJ, Funovits J, Felson DT, et al. (2010) 2010 rheumatoid arthritis classification criteria: an American College of Rheumatology/European League Against Rheumatism collaborative initiative. Annals of the Rheumatic Diseases 69: 1580–1588.

OPEN ACCESS Freely available online PLOS | GENETICS

Genome-Wide Association Study and Gene Expression Analysis Identifies *CD84* as a Predictor of Response to Etanercept Therapy in Rheumatoid Arthritis

Jing Cui[1☯], Eli A. Stahl[1,2,3☯¤a], Saedis Saevarsdottir[4,5], Corinne Miceli[6,7], Dorothee Diogo[1,2,3], Gosia Trynka[1,2,3], Towfique Raj[2,3,8], Maša Umićević Mirkov[9], Helena Canhao[1,10,11], Katsunori Ikari[12], Chikashi Terao[13,14], Yukinori Okada[1,2,3], Sara Wedrén[4,5], Johan Askling[4,15], Hisashi Yamanaka[12], Shigeki Momohara[12], Atsuo Taniguchi[12], Koichiro Ohmura[13], Fumihiko Matsuda[14], Tsuneyo Mimori[13], Namrata Gupta[3], Manik Kuchroo[3,8], Ann W. Morgan[16], John D. Isaacs[17], Anthony G. Wilson[18], Kimme L. Hyrich[19], Marieke Herenius[20], Marieke E. Doorenspleet[20], Paul-Peter Tak[20¤b], J. Bart A. Crusius[21], Irene E. van der Horst-Bruinsma[22], Gert Jan Wolbink[23,24,25], Piet L. C. M. van Riel[9], Mart van de Laar[26], Henk-Jan Guchelaar[27], Nancy A. Shadick[1], Cornelia F. Allaart[28], Tom W. J. Huizinga[28], Rene E. M. Toes[28], Robert P. Kimberly[29], S. Louis Bridges Jr.[29], Lindsey A. Criswell[30], Larry W. Moreland[31], João Eurico Fonseca[10,11], Niek de Vries[20], Barbara E. Stranger[2,3], Philip L. De Jager[2,3,7], Soumya Raychaudhuri[1,2,3,32], Michael E. Weinblatt[1], Peter K. Gregersen[33], Xavier Mariette[6,7], Anne Barton[34], Leonid Padyukov[5], Marieke J. H. Coenen[9], Elizabeth W. Karlson[1], Robert M. Plenge[1,2,3*]

1 Division of Rheumatology, Immunology, and Allergy, Brigham and Women's Hospital, Harvard Medical School, Boston, Massachusetts, United States of America, **2** Division of Genetics, Brigham and Women's Hospital, Harvard Medical School, Boston, Massachusetts, United States of America, **3** Medical and Population Genetics Program, Chemical Biology Program, Broad Institute, Cambridge, Massachusetts, United States of America, **4** Rheumatology Unit, Department of Medicine, Karolinska Institutet and Karolinska University Hospital Solna, Stockholm, Sweden, **5** Institute of Environmental Medicine, Karolinska Institutet, Stockholm, Sweden, **6** Université Paris-Sud, Orsay, France, **7** APHP–Hôpital Bicêtre, INSERM U1012, Le Kremlin Bicêtre, Paris, France, **8** Program in Translational NeuroPsychiatric Genomics, Institute for the Neurosciences, Department of Neurology, Brigham and Women's Hospital, Boston, Massachusetts, United States of America, **9** Department of Human Genetics, Radboud University Nijmegen Medical Centre, Nijmegen, The Netherlands, **10** Rheumatology Research Unit, Instituto de Medicina Molecular, Faculdade de Medicina da Universidade de Lisboa, Lisbon, Portugal, **11** Rheumatology Department, Santa Maria Hospital–CHLN, Lisbon, Portugal, **12** Institute of Rheumatology, Tokyo Women's Medical University, Tokyo, Japan, **13** Department of Rheumatology and Clinical Immunology, Kyoto University Graduate School of Medicine, Kyoto, Japan, **14** Center for Genomic Medicine, Kyoto University Graduate School of Medicine, Kyoto, Japan, **15** Clinical Epidemiology Unit, Department of Medicine, Karolinska Institute/Karolinska University Hospital, Stockholm, Sweden, **16** NIHR–Leeds Musculoskeletal Biomedical Research Unit and Leeds Institute of Molecular Medicine, University of Leeds, Leeds, United Kingdom, **17** Musculoskeletal Research Group, Institute of Cellular Medicine, Newcastle Upon Tyne, United Kingdom, **18** Rheumatology Unit, Medical School, University of Sheffield, Sheffield, United Kingdom, **19** School of Translational Medicine, Arthritis Research UK Epidemiology Unit, University of Manchester, Manchester, United Kingdom, **20** Department of Clinical Immunology and Rheumatology, Academic Medical Center/University of Amsterdam, Amsterdam, The Netherlands, **21** Laboratory of Immunogenetics, Department of Pathology, Vrije Universiteit Medical Center, Amsterdam, The Netherlands, **22** Department of Rheumatology, Vrije Universiteit University Medical Center, Amsterdam, The Netherlands, **23** Sanquin Research Landsteiner Laboratory, Academic Medical Center, University of Amsterdam, Amsterdam, The Netherlands, **24** School of Medicine and Biomedical Sciences, Sheffield University, Sheffield, United Kingdom, **25** Jan van Breemen Institute, Amsterdam, The Netherlands, **26** Arthritis Center Twente, University Twente and Medisch Spectrum Twente, Enschede, The Netherlands, **27** Department of Clinical Pharmacy and Toxicology, Leiden University Medical Center, Leiden, The Netherlands, **28** Department of Rheumatology, Leiden University Medical Centre, Leiden, The Netherlands, **29** Department of Medicine, University of Alabama at Birmingham, Birmingham, Alabama, United States of America, **30** Rosalind Russell Medical Research Center for Arthritis, Division of Rheumatology, Department of Medicine, University of California San Francisco, San Francisco, California, United States of America, **31** Division of Rheumatology and Clinical Immunology, University of Pittsburgh, Pittsburgh, Pennsylvania, United States of America, **32** NIHR Manchester Musculoskeletal Biomedical Research Unit, Central Manchester NHS Foundation Trust, Manchester Academic Health Sciences Centre, Manchester, United Kingdom, **33** The Feinstein Institute for Medical Research, North Shore–Long Island Jewish Health System, Manhasset, New York, United States of America, **34** Arthritis Research UK Epidemiology Unit, Musculoskeletal Research Group, University of Manchester, Manchester Academic Health Sciences Centre, Manchester, United Kingdom

Abstract

Anti-tumor necrosis factor alpha (anti-TNF) biologic therapy is a widely used treatment for rheumatoid arthritis (RA). It is unknown why some RA patients fail to respond adequately to anti-TNF therapy, which limits the development of clinical biomarkers to predict response or new drugs to target refractory cases. To understand the biological basis of response to anti-TNF therapy, we conducted a genome-wide association study (GWAS) meta-analysis of more than 2 million common variants in 2,706 RA patients from 13 different collections. Patients were treated with one of three anti-TNF medications: etanercept (n = 733), infliximab (n = 894), or adalimumab (n = 1,071). We identified a SNP (rs6427528) at the *1q23* locus that was associated with change in disease activity score (ΔDAS) in the etanercept subset of patients ($P = 8\times10^{-8}$), but not in the infliximab or adalimumab subsets ($P > 0.05$). The SNP is predicted to disrupt transcription factor binding site motifs in the 3′ UTR of an immune-related gene, *CD84*, and the allele associated with better response to etanercept was associated with higher *CD84* gene expression in peripheral blood mononuclear cells ($P = 1\times10^{-11}$ in 228 non-RA patients and $P = 0.004$ in 132 RA patients). Consistent with the genetic findings, higher *CD84* gene expression correlated with lower cross-sectional DAS ($P = 0.02$, n = 210) and showed a non-significant trend for better ΔDAS in a subset of RA patients with gene expression data (n = 31, etanercept-treated). A small, multi-ethnic replication showed a non-significant trend towards an association among etanercept-treated RA patients of Portuguese ancestry (n = 139, $P = 0.4$), but no association among patients of Japanese ancestry (n = 151, $P = 0.8$). Our study demonstrates that an allele associated with response to etanercept therapy is also associated with *CD84* gene expression, and further that *CD84* expression correlates with disease activity. These findings support a model in which *CD84* genotypes and/or expression may serve as a useful biomarker for response to etanercept treatment in RA patients of European ancestry.

Citation: Cui J, Stahl EA, Saevarsdottir S, Miceli C, Diogo D, et al. (2013) Genome-Wide Association Study and Gene Expression Analysis Identifies *CD84* as a Predictor of Response to Etanercept Therapy in Rheumatoid Arthritis. PLoS Genet 9(3): e1003394. doi:10.1371/journal.pgen.1003394

Editor: Alison Motsinger-Reif, North Carolina State University, United States of America

Received August 13, 2012; **Accepted** January 13, 2013; **Published** March 28, 2013

Funding: JC is supported by grants from ACR REF HPNIA award and the NIH (R01-AR059073, P60-AR047782, U01-GM092691, R01-AR049880). RMP is supported by grants from the NIH (R01-AR057108, R01-AR056768, U01-GM092691, R01-AR059648) and holds a Career Award for Medical Scientists from the Burroughs Wellcome Fund. The American College of Rheumatology Research and Education Foundation provided funding to support this project. The eRA study was supported by R01 AI/AR47487. SS's work was supported by a clinical research fund from Stockholm County (ALF fund). LP's work was supported by the Swedish Rheumatism Association and the Swedish Medical Research Council. NdV and MED were sponsored by CTMM, the Center for Translational Molecular Medicine, and the Dutch Arthritis Foundation project TRACER (grant 04I-202). The Swedish studies (EIRA, Karolinska) were supported by grants from the Swedish Medical Research Council, the Stockholm County Council, the Swedish Council for Working Life and Social Research, King Gustaf V's 80-year foundation, the Swedish Rheumatism Association, the Swedish Foundation for Strategic Research, the Swedish COMBINE project, and the IMI funded BTCure project. The funders had no role in study design, data collection and analysis, decision to publish, or preparation of the manuscript.

Competing Interests: The authors have declared that no competing interests exist.

* E-mail: rplenge@partners.org

¤a Current address: Division of Psychiatric Genomics, Mt. Sinai School of Medicine, New York, New York, United States of America
¤b Current address: GlaxoSmithKline, Stevenage, United Kingdom

◑ These authors contributed equally to this work.

Introduction

Rheumatoid arthritis (RA) is an autoimmune disease characterized by chronic inflammation of the synovial lining of the joint [1]. If left untreated, outcome varies from self-limited disease in a small proportion of RA patients to severe disease resulting in profound structural damage, excess morbidity and disability, and early mortality [2]. In the last twenty years, disease activity has been controlled in many patients by treatment with disease-modifying anti-rheumatic drugs (DMARDs), such as methotrexate, and the more recently developed biologic DMARDs that block inflammatory cytokines such as tumor necrosis factor-alpha (TNFa) [3]. Unfortunately, these medications are not effective in all RA patients, with up to one-third of patients failing to respond to any single DMARD [1–3]. Moreover, the biological mechanisms underlying treatment failure are unknown, which limits the development of clinical biomarkers to guide DMARD therapy or the development of new drugs to target refractory cases.

There are two classes of anti-TNF therapy: the TNF receptor fusion protein (etanercept), which acts as a soluble receptor to bind circulating cytokine and prevent TNF from binding to its cell surface receptor, and monoclonal antibodies that bind TNF (adalimumab, infliximab, certolizumab, and golimumab). There are undoubtedly shared mechanisms between the two drug classes (e.g., downstream signaling factors), as illustrated by similar effects on the change in inflammatory cytokines, complement activation, lymphocyte trafficking, and apoptosis [4,5,6]. Similarly, there are likely to be different biological factors that influence response: infliximab and adalimumab are approved for treatment of Crohn's disease; infliximab and adalimumab bind to transmembrane TNF on the surface of activated immune cells, whereas etanercept only binds soluble TNF [7]; and etanercept also binds a related molecule, lymphotoxin alpha (LTA), whereas infliximab/adalimumab do not [8].

Pharmacogenetics of response to anti-TNF therapy in RA remains in its early stages, with no single variant reaching an unambiguous level of statistical significance. Candidate gene studies suggest associations of TNFa or TNF receptor alleles, RA risk alleles or other SNPs with response to anti-TNF therapy [9,10,11]. Two GWAS in small sample sets (largest was 566 patients) have been performed, which identified loci with suggestive evidence for association [12,13]. Therefore, GWAS of large sample sizes may yet uncover genetic factors associated with response to anti-TNF therapy in RA, and larger cohorts enable separate analyses of the different types of anti-TNF drugs.

Here we report a GWAS of 2,706 samples with anti-TNF treatment response data collected from an international collaboration, including previously published GWAS data [12,13]. Our primary outcome measure was the change in disease activity score based on a joint count in 28 joints (DAS28) from baseline to 3–12 months after initiating anti-TNF therapy. Our secondary outcome measure was European League Against Rheumatism (EULAR) responder status [14,15], where patients are classified as EULAR good responders, moderate responders or non-responders based on follow up DAS28 after treatment and overall change in DAS28. We found a highly significant association for a variant that we also show is also a strong expression quantitative trait locus (eQTL) for the *CD84* gene. Our findings suggest that *CD84* genotype and/or expression may prove to be a biomarker for etanercept response in RA patients.

Results

Genome-wide association study

Clinical and GWAS data were compiled for 2,706 individuals of European ancestry from 13 collections as part of an international collaboration. Table 1 shows sample sizes, phenotypes and clinical variables for the four collections that were the units of analysis (additional details are shown in Table S1). Disease activity score based on a 28-joint count (DAS28) were collected at baseline and at one time point after anti-TNF therapy administration (mean 3.7 months, range 3–12 months). We defined our primary phenotype

Author Summary

There are no genetic predictors of response to one of the most widely used classes of drugs in the treatment of rheumatoid arthritis—biological modifiers of the inflammatory cytokine tumor necrosis factor-alpha (or anti-TNF therapy). To identify genetic predictors, we performed the largest genome-wide association study (GWAS) to date as part of an international collaboration. In our study, which included 2,706 RA patients treated with one of three anti-TNF drugs, the most significant finding was restricted to RA patients treated with etanercept ($P = 8 \times 10^{-8}$), a drug that acts as a soluble receptor to bind circulating cytokine and prevents TNF from binding to its cell surface receptor. The associated variant influences expression of a nearby immune-related gene, *CD84*, whose expression is correlated with disease activity in RA patients. Together, our data support a model in which genomic factors related to *CD84* expression serve as a predictor of disease activity and response to etanercept therapy among RA patients of European ancestry, but not anti-TNF therapies that act through different biological mechanisms or potentially in RA patients of other genetic ancestries.

as a change in DAS28 (ΔDAS) from baseline (so that greater ΔDAS corresponded with better response to therapy; overall mean and standard deviation of 2.1±1.3), adjusted for baseline DAS. A secondary phenotype was used based on European League Against Rheumatism (EULAR) response criteria. EULAR 'good response' was defined as ending DAS<3.2 and ΔDAS>1.2; 'non-response' was defined as ΔDAS <0.6 or ΔDAS≤1.2, and ending DAS >5.1; and 'moderate response' is in between [15]. We limited our secondary analysis to a dichotomous outcome, EULAR good responders (n = 998 for all patients treated with anti-TNF therapy) versus EULAR non-responders (n = 655), excluding the moderate category based on the hypothesis that a more extreme phenotype of response would yield improved discrimination.

Clinical variables were examined for association with phenotype, and therefore possible confounding in genetic association tests. In multivariate models (Table S2), only baseline DAS was strongly associated with the ΔDAS phenotype. As previously shown [11], age and gender showed univariate associations that were attenuated in the multivariate analysis. Accordingly, we used only baseline DAS as a clinical covariate, as this allowed us to maximize sample size given clinical variable missing data in some cohorts.

We performed quality control (QC) filtering and data processing of GWAS data for each of eleven genotyping batches. Genotyping array platforms are described in the Methods. HapMap2 imputation allowed us to test for association at >2 M SNPs with imputation quality scores >0.5. Genotype data were merged across several genotype batches to create four collections for genome-wide association testing. We performed linear regression association tests using baseline DAS and three principal components as covariates, and performed inverse-variance weighted meta-analysis to combine results across the four collections. Quantile-quantile plots with genomic control λ_{GC} values are shown in Figure S1. We found no evidence of systematic inflation of association test results, and no evidence of deflation for imputed versus genotyped SNPs. As a final filter, we excluded SNPs that

Table 1. Samples and clinical data.

Collection (analysis batch):	REF	BRAGGSS	DREAM	ReAct	Total
Sample sizes	959*	595	880*	272	2706
Drug subsets					
etanercept	365	259	109	0	733
infliximab	415	268	211	0	894
adalimumab	174	68	557	272	1071
EULAR Reponse categories					
Good responder	432**	161	313	92	998
Moderate responder	243	258	359	131	991
Non-responder	322	176	208	49	755
Genotype platform	mixed	Affy 500K	Illu550K +650K	Illumina OmniExpress	
Clinical variables					
Age, yr; mean (SD)	53.6 (12.7)	57.4 (10.9)	54.8 (12.9)	53.9 (10.8)	
Disease duration, yr; mean (SD)	6.7 (9.4)	14 (9.8)	9.6 (9.5)	12 (9.1)	
Gender, female %	75.6	77.3	68.3	77.9	
Seropositive, %	87	78	80	70	
MTX co-therapy, %	65.6	85.6	76.0	50.0	
Baseline DAS, mean (SD)	5.5 (1.2)	6.7 (0.9)	5.5 (1.2)	5.9 (1.0)	
ΔDAS, mean (SD)	1.9 (1.6)	2.5 (1.5)	1.9 (1.3)	2.2 (1.3)	
Mean treatment duration	4.6	5.6	3	3	
Study design	All***	Observational	Observational	Observational	

*8 patients had no TNF drug information.

**38 patients had only EULAR response (good, moderate or none) clinical data.

***ABCoN, GENRA are prospective cohorts, BeSt, eRA and TEAR are randomized controlled trial (RCT), and rest of REF group are observational cohorts.

doi:10.1371/journal.pgen.1003394.t001

showed strong evidence of heterogeneity across collections (Cochran's Q P<0.001).

We first analyzed all samples together (n = 2,706), regardless of drug type. We found no clear evidence of association with treatment response measured by ΔDAS (Figure 1A). Similar results were obtained using the binary phenotype of EULAR responder versus EULAR non-responder status (Figures S1 and S2).

We next separately analyzed patients treated with either etanercept (n = 733), infliximab (n = 894) or adalimumab (n = 1,071) (Figure 1B–1D), under the hypothesis that different genetic loci affect response to the different drugs based on their mechanism of action or other biochemical properties. GWAS results are publicly available for all SNPs tested at the Plenge laboratory and RICOPILI Web sites (see URLs). GWAS results for all SNPs achieving $P<10^{-6}$ from any analysis are detailed in the Table S3.

For etanercept-treated RA patients, a locus on chromosome *1q23* achieved near-genome-wide significance (rs6427528, $P_{META} = 8\times10^{-8}$) (Figure 1B, Figure 2A, and Figure 3), but not in the infliximab or adalimumab subsets (*P*>0.05) (Figure S3). SNPs in linkage disequilibrium (LD) showed consistent association results (rs1503860, $P = 1\times10^{-7}$, $r^2 = 1$ with rs6427528 in HapMap; three perfect-LD clusters of SNPs exemplified by rs3737792, rs10908787 and rs11265432 respectively; $P<5\times10^{-6}$; $r^2 = 0.83$, 0.63 and 0.59 with rs6427528, respectively). No single collection was responsible for the signal of association, as the effect size was consistent across all collections (Figure S4). The top SNP rs6427528 was genotyped in the ReAct dataset (Illumina Omni Express genotyping chip), and was well imputed across all other datasets (imputation quality score INFO ≥0.94, which is an estimate of genotype accuracy; the range of INFO scores is 0–1, where 1 indicates high confidence). All of these SNPs had minor

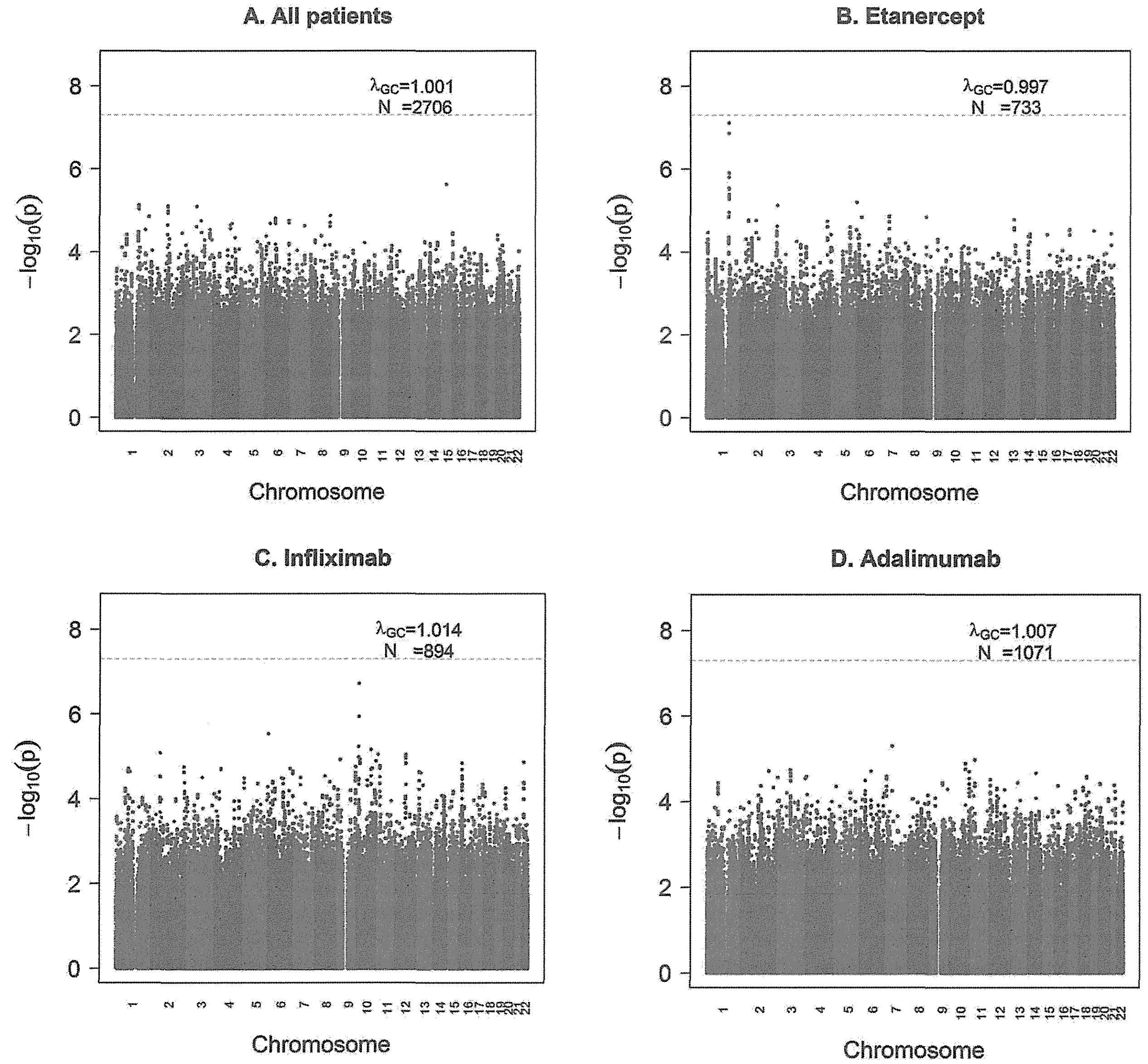

Figure 1. GWAS results for the ΔDAS phenotype. Shown are strengths of association (−Log10 P-value) for each SNP versus position along chromosomes 1 to 22. A) All samples (n = 2,706). B) Etanercept-treated patients (n = 733). C) Infliximab-treated patients (n = 894). D) Adalimumab-treated patients (n = 1,071).
doi:10.1371/journal.pgen.1003394.g001

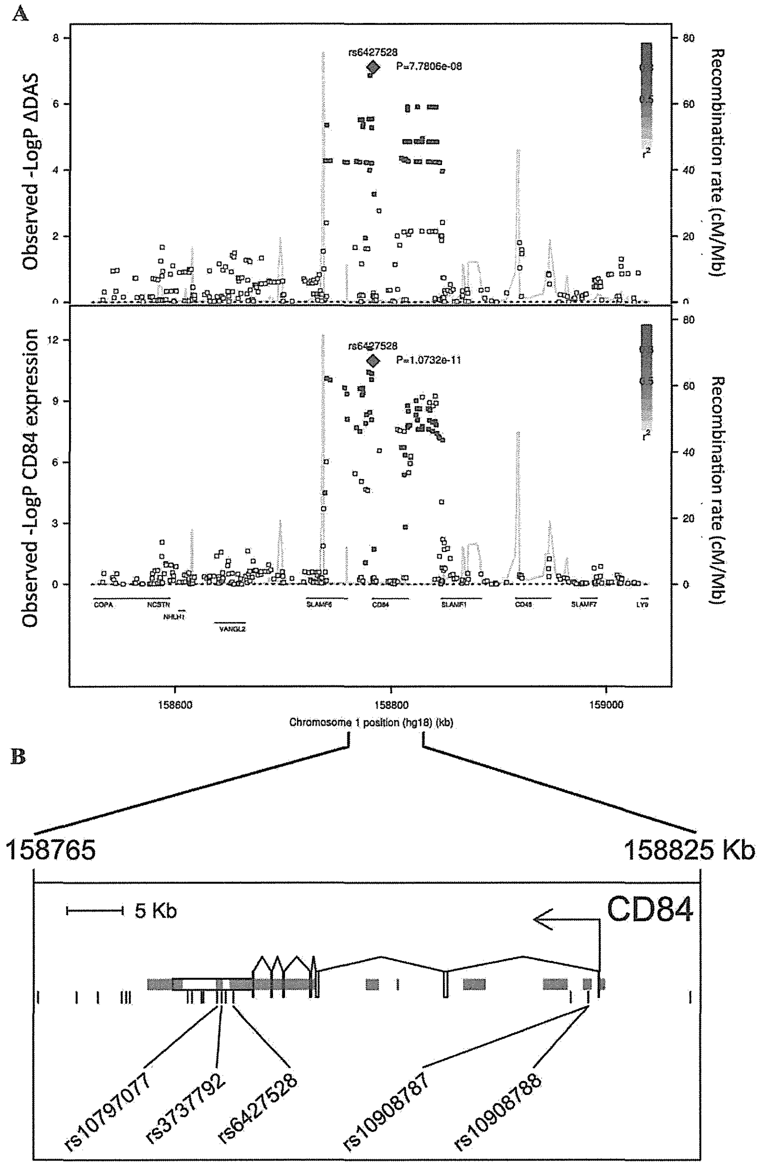

C.

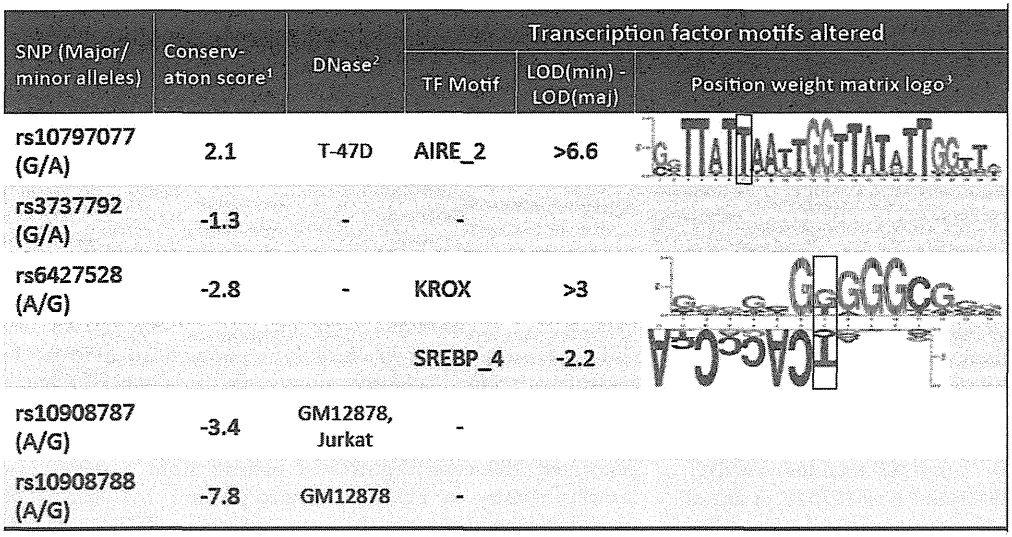

SNP (Major/ minor alleles)	Conservation score[1]	DNase[2]	Transcription factor motifs altered		
			TF Motif	LOD(min) - LOD(maj)	Position weight matrix logo[3]
rs10797077 (G/A)	2.1	T-47D	AIRE_2	>6.6	
rs3737792 (G/A)	-1.3	-	-		
rs6427528 (A/G)	-2.8	-	KROX	>3	
			SREBP_4	-2.2	
rs10908787 (A/G)	-3.4	GM12878, Jurkat	-		
rs10908788 (A/G)	-7.8	GM12878	-		

Figure 2. Association results and SNP annotations in the *1q23 CD84* locus. A) Regional association plots with ΔDAS (top panel) and with *CD84* expression (bottom panel), showing strengths of association (−Log10 P-value) versus position (Kb) along chromosome 1. B) Schematic of *CD84* gene structure (RefSeq gene model, box exons connected by diagonal lines, arrow indicates direction of transcription) with strong enhancer chromatin states (orange rectangles) and SNPs in high LD (r2>0.8) with rs6427528 (vertical ticks). SNPs in enhancers are labeled below. C) Annotations of strong-enhancer rs6427528 proxy SNPs; listed are SNP rs-ID (major and minor alleles), conservation score, cell line with DNAse footprint if present, and transcription factor binding sites altered. 1- Genomic evolutionary rate profiling (GERP) conservation score, where a score >2 indicates conservation across mammals. 2- DNase footprint data are compiled from publicly available experiments by HaploReg. 3- Position weight matrix logos show transcription factor consensus binding sites with nucleotide bases proportional to binding importance. SNP position is boxed. Note that the rs10797077 AIRE_2 and the rs6427528 SREBP_4 motifs are on the minus strand (base complements correspond to SNP alleles), with the SREBP motif shown upside down to align with the rs6427528 KROX motif on the positive strand. Data are from HaploReg.
doi:10.1371/journal.pgen.1003394.g002

allele frequencies ranging from 7–10%. The SNP explains 2.6% variance in response to etanercept treatment.

For patients treated with infliximab, we observed a suggestive result on chromosome *10p14* (rs12570744, $P = 2\times10^{-7}$). No highly significant or suggestive results were observed for the ΔDAS phenotype in patients treated with adalimumab ($P_{META} > 10^{-5}$).

Qualitatively similar results were attained in the analysis of our secondary phenotype, EULAR good responder vs non-responder status (Figures S1 and S2). For SNPs at the *1q23* locus, the pattern of association with responder/non-responder status (etanercept-treated patients) was consistent with the results for ΔDAS ($P = 6\times10^{-3}$ for rs6427528 and rs1503860). We also identified potential novel associations, with suggestive results for infliximab (rs4336372, chromosome *5q35*, $P = 8\times10^{-7}$) and adalimumab (rs940928, chromosome *2q12*, $P = 2\times10^{-6}$).

eQTL and sequence analysis of the *CD84* gene

For each SNP with $P < 10^{-6}$ identified by our GWAS (n = 6 independent SNPs), we searched for biological evidence to support a true positive association. We used genome-wide sequence data from the 1000 Genomes Project to search for putative functional variants in LD with the index SNP (defined as SNPs predicted to change protein-sequence or mRNA splicing). We also used genome-wide expression data to search for an expression quantitative trait locus (eQTL) in public databases and in peripheral blood mononuclear cells (PBMCs) in 228 non-RA patients and in 132 RA patients.

While we did not identify any variants disrupting protein-coding sequences or mRNA splicing, we did find that the *1q23* SNP associated with response to etanercept therapy was a strong eQTL in PBMCs (Figure 2A and Figure 3). In an analysis of 679 SNPs for cis-regulated expression of five genes in the region of LD (*SLAMF6*, *CD84*, *SLAMF1*, *CD48*, and *SLAMF7*), we found that rs6427528-*CD84* (and SNPs in LD with it) was the top eQTL of all results (n = 228 subjects; Figure 2A). This SNP was specifically associated with *CD84* expression, and was not an eQTL for other genes in the region (P>0.36 for the other genes).

We replicated our eQTL finding in 132 RA patients with both GWAS data and genome-wide expression data. PBMC expression data were available from RA patients in the Brigham RA Sequential Study (BRASS) and Autoimmune Biomarkers Collaborative Network (ABCoN) collections. We observed a significant association between rs6427528 genotype and *CD84* expression (linear regression adjusted for cohort P = 0.004, rank correlation P = 0.018). The direction of effect was the same as in the PBMC samples from 228 non-RA patients. A combined analysis of RA patients and the non-RA patient eQTL data (described above) yielded rank correlation $P = 3\times10^{-10}$ (n = 360 total individuals).

We searched sequence data to determine if rs6427528, or any of the SNPs in LD with it, were located within conserved, non-coding motifs that might explain the eQTL data. We used HaploReg [16] to examine the chromatin context of rs6427528 and 26 SNPs in LD with it (at $r^2 > 0.50$). We found that 5 SNPs occur in strong enhancers inferred from chromatin marks (Figure 2B) [17]. Two of these 5 SNPs, rs10797077 and rs6427528 ($r^2 = 0.74$ to each other), are predicted to disrupt transcription factor binding sites, and rs10797077 occurs at a site that shows conservation across mammalian genomes [18]. Figure 2C shows the DNA sequence position weight matrices of the transcription factor binding sites changed by rs10797077 (the minor allele creates a stronger binding site for the AIRE transcription factor) and rs6427528 (the minor allele creates a binding site for KROX and SREBP).

Expression of *CD84* as a biomarker of disease activity and treatment response

Because the genetic data demonstrates that the allele associated with better response is associated with higher *CD84* expression, this suggests that *CD84* expression itself may serve as a useful biomarker of disease activity or treatment response. We tested both hypotheses using PBMC expression data from the BRASS and ABCoN collections. First, we tested if *CD84* expression is associated with cross-sectional DAS, adjusting for age, gender and cohort (Figure 4). We observed a significant inverse association between *CD84* expression and cross-sectional DAS in 210 RA patients (beta = −0.3, P = 0.02, $r^2 = 0.02$). That is, higher *CD84* expression was associated with lower DAS, regardless of treatment.

Second, we tested *CD84* for association with our primary treatment response phenotype, ΔDAS. The sample size for this analysis was smaller than for the cross-sectional analysis, as we required that patients be on anti-TNF therapy and have pre- and post-treatment DAS. We found that *CD84* expression levels showed a non-significant trend towards an association with ΔDAS in 31 etanercept-treated patients (beta = 0.2, $r^2 = 0.002$, P = 0.46) and in all 78 anti-TNF-treated patients (beta = 0.14, $r^2 = 0.004$, P = 0.4). The effect is in the same direction one would predict based on the genetic association at rs6427528: the allele associated with better response is also associated with higher *CD84* expression (Figure 3), and in 31 RA patients, higher *CD84* expression (regardless of genotype) is associated with a larger ΔDAS (i.e., better response; Figure 4).

Replication of genetic data in a small, multi-ethnic cohort

Since most of the samples available to us as part of our international collaboration were included in our GWAS, few additional samples were available for replication. In addition, the remaining samples available to us were from different ethnic backgrounds. Nonetheless, we sought to replicate the associations of rs6427528 with ΔDAS in these additional samples. We genotyped 139 etanercept-treated patients from a rheumatoid arthritis registry in Portugal (Reuma.pt) and 151 etanercept-treated patients from two Japanese collections (IORRA, n = 88 patients on etanercept and Kyoto University, n = 63 on etanercept). Replication sample sizes, clinical data and results for these

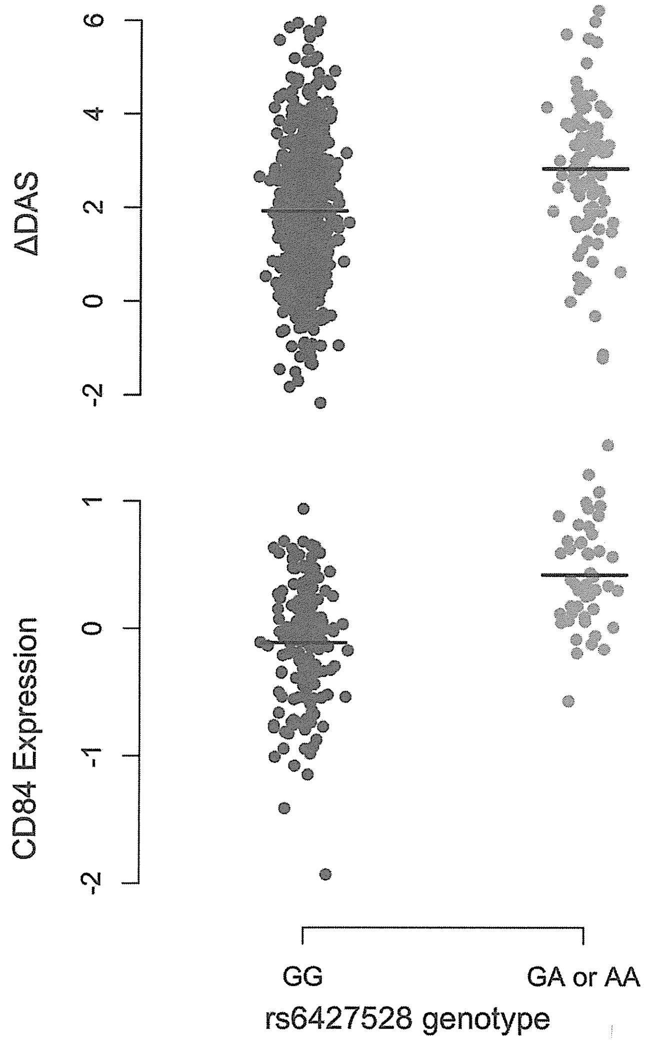

Figure 3. *1q23/CD84* genotype association plots for ΔDAS and *CD84* gene expression. Shown are ΔDAS in our GWAS in etanercept-treated patients (top panel, n = 733; n = 634 with the GG genotype and n = 99 with the GA or AA genotype) and *CD84* expression in our eQTL results (bottom panel, n = 228 non-RA patients; n = 178 with the GG genotype and n = 50 with the GA or AA genotype). The rare-allele homozygous genotype AA was observed four times in our ΔDAS GWAS and was pooled with the heterozygous GA genotype for this figure; AA homozygotes were not observed in the *CD84* eQTL data. Association analyses reported in the text regressed phenotype (ΔDAS, $P = 8\times10^{-8}$; *CD84* expression, $P = 1\times10^{-11}$) on minor-allele dosage (range 0–2).
doi:10.1371/journal.pgen.1003394.g003

two SNPs are shown in Table S4. Based on the observed effect size in the GWAS and observed allele frequency in the replication samples, we had 32% power to replicate this finding in the Portuguese samples and 17% power to replicate this finding in the Asian samples at $P<0.05$. The same association analysis as for GWAS was carried out: linear regression assuming an additive genetic model and using ΔDAS as phenotype, adjusted for baseline DAS. Replication results are shown in Figure 5.

While the SNPs fail to replicate in these patient collections at $P<0.05$, the direction of effect is the same in the Portuguese and Kyoto replication samples as in our GWAS. In a combined analysis limited to subjects of European-ancestry (GWAS data and Portuguese replication samples), rs6427528 remained highly suggestive ($P = 2\times10^{-6}$). Including the Japanese subjects, the overall GWAS+replication combined meta-analysis P-value remained suggestive ($P = 5\times10^{-4}$).

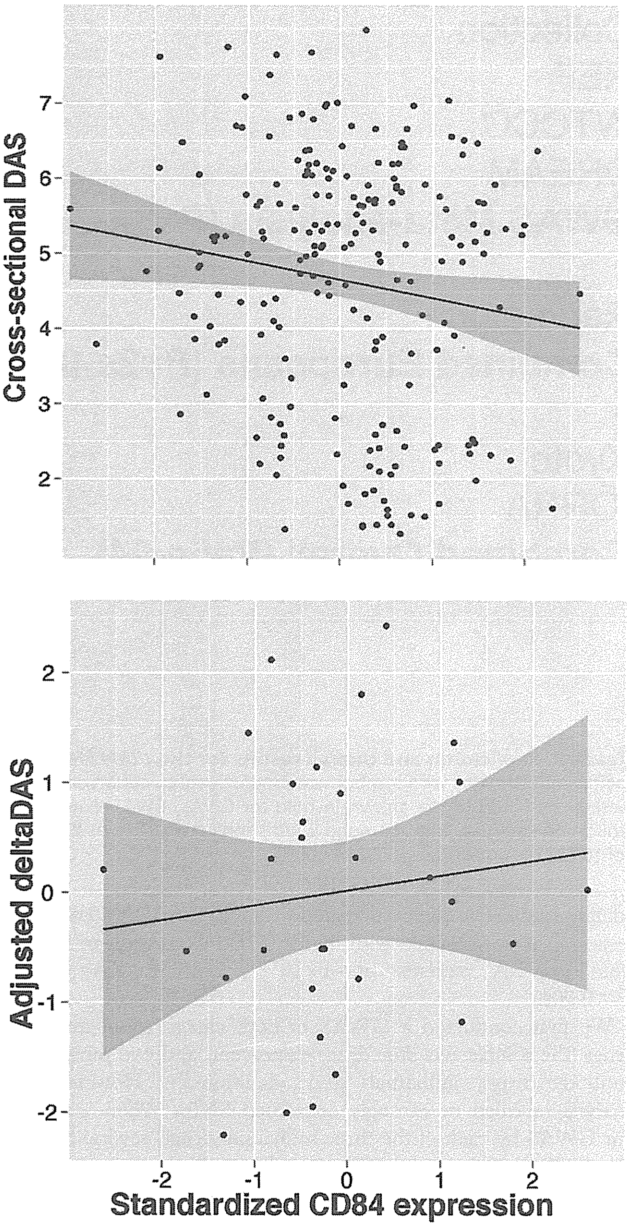

Figure 4. *CD84* expression level and clinical features. Analyses are shown in RA patients from the BRASS and ABCoN registries, for baseline DAS (top panel, n = 210; $R^2 = 0.02$, p = 0.02) and ΔDAS (bottom panel, n = 31; $R^2 = 0.001$, p = 0.46). Best-fit linear regression lines are shown in black, with shaded regions showing linear regression model (slope and intercept) 95% confidence intervals. *CD84* expression levels were quantile normalized, and ΔDAS values were adjusted for age, gender and baseline DAS.
doi:10.1371/journal.pgen.1003394.g004

Discussion

Here we present the largest GWAS to date on anti-TNF therapy response in 2,706 RA patients. We find a significant association at the *1q23/CD84* locus in 733 etanercept treated patients ($P = 8\times10^{-8}$), but not in RA patients treated with drugs that act as a monoclonal antibody to neutralize TNF (infliximab or

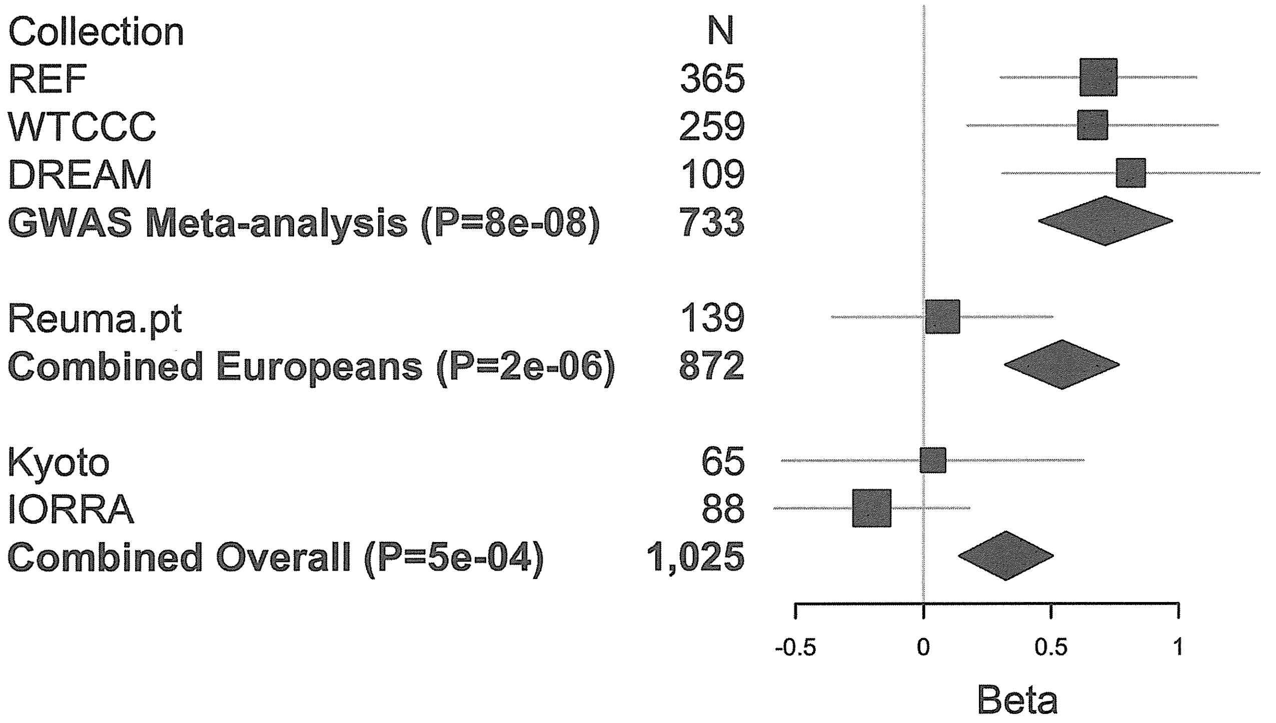

Figure 5. Replication and overall results for the *CD84* SNP rs6427528. Forest plot shows each cohort, sample size and linear regression beta coefficient estimates with symbol size proportional to cohort sample size and thin horizontal lines showing beta 95% CIs. Inverse variance weighted meta-analysis results are shown in bold for GWAS, GWAS+European (Portuguese) replication samples, and for GWAS+European+Asian (Japanese) replication samples, with diamond widths indicating beta 95% CIs.
doi:10.1371/journal.pgen.1003394.g005

adalimumab). The allele associated with a larger ΔDAS (i.e., better response) was associated with higher *CD84* expression in PBMCs from non-RA patients ($P = 1 \times 10^{-11}$) and in RA patients ($P = 0.004$).

We first conducted a GWAS of both categories of anti-TNF drugs (the soluble receptor drug, etanercept, and two monoclonal antibody drugs, infliximab and adalimumab). However, this analysis revealed no strongly associated SNPs. When we subset our GWAS by each of the three individual drugs, several SNPs in the *1q23* locus were highly significant in etanercept-treated patients, and SNPs in three other loci (*10p15*, *5q35* and *2q12*) were associated in infliximab or adalimumab subset analyses. Furthermore, the top SNPs for each analysis (Table S3) showed little correlation across the three anti-TNF drugs. This simple observation suggests that genetic control of treatment response may be different for different drugs. This finding is consistent with the clinical observation that RA patients who fail one anti-TNF drug may still respond to a different anti-TNF drug, albeit at lower rates of response [19]. If confirmed in larger samples and more comprehensive analyses, then this could have major implications for how physicians prescribe these drugs.

The most significant finding from our GWAS was a set of equivalent SNPs in LD with each other from the *1q23* locus in etanercept-treated RA patients (Figure 1 and Figure 2A). While the top SNP did not reach genome-wide significance in predicting treatment response, it did reach genome-wide significance as an eQTL in PBMCs ($P = 1 \times 10^{-11}$; Figure 2A). This finding indicates that the SNP (or another variant in LD with it) is indeed biologically functional in a human tissue that is important in the immune response. Two SNPs, rs10797077 and rs6427528, disrupt transcription factor binding sites, and represent excellent candidates for the causative allele to explain the effect on *CD84* expression (Figure 2C).

Our findings suggest that *CD84* genotype and/or expression could be a biomarker for etanercept treatment response among individuals of European ancestry. The genetic and expression data predict that *CD84* expression should be positively associated with treatment response (i.e., higher expression is associated with better response; Figure 3). While we did not observe a significant association between *CD84* levels and ΔDAS, we did observe a trend consistent with this prediction (Figure 4). Importantly, we note that power was extremely limited with the small sample sizes for which we had *CD84* expression as well as drug response data (n = 31 RA patients treated with etanercept).

The *CD84* gene is a compelling candidate for immune response, belonging to the CD2 subset of the immunoglobulin superfamily. It has been implicated in T-cell activation and maturation [20]. CD84 localizes to the surface of CD4+ and CD8+ T cells, and acts as a costimulatory molecule for IFN-gamma secretion [21]. *CD84* is also expressed in B-cells, monocytes and platelets. *CD84* has not been previously implicated in genetic studies of RA risk, disease activity, disease severity, or treatment response.

A limitation of our study is the small sample size available for replication (n = 290 etanercept-treated patients), and the lack of replication observed for the top *CD84* SNP (rs6427528) among patients of Portuguese and Japanese ancestry. The simplest explanation is that our original observation in the GWAS data represents a false positive association. However, the eQTL and gene expression data argue against this possibility. Explanations for a false negative finding in our replication collections include: (1) lack of power, especially if the effect size observed in the GWAS represents an over-estimate of the true effect size (the Winner's Curse) – we estimate that we had 32% and 17% power (at $P = 0.05$) to detect an association in the Portuguese and Japanese sample collections, respectively; (2) clinical heterogeneity, which is always a possibility in pharmacogenetic studies, especially those conducted in different countries; and (3) ethnic differences, including different patterns of LD between the underlying causative allele (which is as yet unknown) and marker SNPs tested in our study. We did observe subtle differences in local patterns of LD between Asians and Europeans using genetic data from the 1000 Genomes Project (Figure S5). We note that the rs6427528 minor allele A has a frequency of ~5–10% in European and East Asian populations, and ~50% in the African YRI population (HapMap2 and 1000 Genomes); therefore, it may be of interest to test African American samples in replication.

What are the options for increasing sample size in pharmacogenetic studies, thereby providing an opportunity to replicate our *CD84* genetic and expression findings? While it might seem trivial to collect more samples through traditional registries, this is extremely challenging for phenotypes pertaining to treatment efficacy. To underscore this point, we highlight our study design, where we organized samples and clinical data from 16 different collections across 7 different countries in order to obtain the samples for the current study. Going forward, non-traditional strategies to collect biospecimens linked with clinical data (e.g., online registries, electronic medical records) may be required to achieve clinical collections of sufficient size to discover pharmacogenomic predictors of efficacy.

In conclusion, we conducted the largest GWAS to date for response to anti-TNF therapy in RA patients. Our genetic and expression data suggest that *CD84* genetic variants and/or expression levels could be developed as predictive biomarkers for etanercept treatment response in RA patients of European ancestry.

Methods

Samples and clinical data

All patients met 1987 ACR criteria for RA, or were diagnosed by a board-certified rheumatologist. In addition, patients were required to have at least moderate disease activity at baseline (DAS>3.2). All patients gave their informed consent and all institutional review boards approved of this study. A total of 13 collections from across 5 countries were included in GWAS [11,12,13,22]: Autoimmune Biomarkers Collaborative Network (ABCoN) from the U.S. (N = 79); the Genetics Network Rheumatology Amsterdam (GENRA, N = 53); the Dutch Behandelstrategieen voor Rheumatoide Arthritis (BeSt, N = 85); the U.K. Biological in Rheumatoid arthritis Genetics and Genomics Study Syndicate (BRAGGSS, N = 140); the U.S. Brigham Rheumatoid Arthritis Sequential Study (BRASS, N = 55); the Swedish Epidemiological Investigation of Rheumatoid Arthritis (EIRA, N = 298); the Immunex Early Rheumatoid Arthritis study (eRA N = 57); the Swedish Karolinska Institutet study (KI, N = 77); the Netherlands collection from Leiden University Medical Center (LUMC, N = 43); and the U.S. Treatment of Early Aggressive RA (TEAR, N = 109). We refer to these collections as the American College of Rheumatology Research and Education Foundation (REF) collection, as funding for GWAS genotyping was provided by the "*Within Our Reach*" project. We included additional samples from BRAGGSS (N = 595) [12]; the Dutch Rheumatoid Arthritis Monitoring registry (DREAM) in the Netherlands, and the ApotheekZorg (AZ) database (which facilitates the Dutch distribution of adalimumab; N = 880) [23,24], together referred to as DREAM; and the French Research in Active Rheumatoid Arthritis (ReAct, N = 272) [25].

Additional samples were collected for replication of SNPs in the *1q23* locus. These included the Rheumatic Diseases Portuguese Register (Reuma.pt, N = 378) from the Portuguese Society of Rheumatology (SPR), which captures more than 90% of patients treated with biological therapies and managed in rheumatology departments across Portugal [26]. Additional replication samples (N = 374) of East Asian ancestry were included from the IORRA and Kyoto University Hospital registries, part of the Japanese Genetics and Allied research in Rheumatic diseases Networking consortium (GARNET) [27].

Clinical data were collected in each cohort, including disease activity scores at baseline and at least one time point after treatment, gender, age, methotrexate use, as well as autoantibody status (RF or CCP). The composite disease activity scores for 28 joints (DAS28) included laboratory values for erythrocyte sedimentation rate (ESR) for most samples and C-reactive protein (CRP) for 191 samples in the REF collection (ABCoN, BRASS and eRA cohorts). DAS28 values were available at baseline and at 3–12 months after initiating anti-TNF therapy. Our primary phenotype was defined as ΔDAS = baseline DAS - end DAS, and responder status was also determined according to EULAR criteria for start and end DAS [15]. Clinical variables were assessed for association with phenotype in multivariate linear or logistic regression models for both the ΔDAS and EULAR responder-status phenotypes. Clinical variables that were significant in these analyses were retained as covariates in genetic association tests, except for methotrexate co-therapy. Including a covariate for methotrexate co-therapy reduced sample size substantially due to missing clinical data, so results were compared for our primary analysis and a secondary analysis with the covariates (and with reduced sample size) and the results were verified not to be impacted (not shown).

Genotyping and data processing

A total of eleven genotyping batches were processed separately. (1) BRASS samples were genotyped using Affymetrix 6.0 chip [28]; (2) WTCCC samples were genotyped on Affymetrix 500K chip [12]. All other cohorts were genotyped using Illumina platform arrays (see Table 1). Our American College of Rheumatology Research Education Fund (REF) collection was made up of smaller cohorts from throughout North America and Europe, including BRASS samples. Also included in REF: (3) ABCoN [13] and (4) EIRA [29] were separately genotyped on the Illumina 317K genotyping array; (5) eRA on the Illumina 550K chip; and (6) GENRA, BeSt, BRAGGSS (a subset of N = 53 samples), KI and LUMC were genotyped in one batch, and (7) BRAGGSS (N = 87) and TEAR were genotyped in a second batch, both using Illumina 660k chips, at the Broad Institute (8–10). DREAM and AZ samples were genotyped in three batches, one on 550K chip and two on 660K chips (manuscript in preparation), and (11) ReAct samples were genotyped on Illumina OmniExpress chips. Quality control (QC) filtering was done in each genotyping batch, including filtering individuals with >5% missing data, and filtering SNPs with >1% missing data, minor allele frequency (MAF) <1% and Chi-squared test of Hardy Weinberg equilibrium $P_{HWE}<10^{-5}$. We then used individual-pairwise identity-by-state estimates to remove occasional related and potentially contaminated samples. Data processing and QC were performed in PLINK [30]. Principal Components Analysis (PCA) was performed using EIGENSTRAT [31] (default settings) on the combined dataset using 20,411 SNPs genotyped across all datasets. Ethnicity outliers including all individuals of non-European decent were identified and removed, and the first three eigenvectors were used as covariates in GWAS.

Imputation was conducted on each of eleven datasets separately, using the IMPUTE v1 software [32] and haplotype-phased

HapMap Phase 2 (release 22) European CEU founders as a reference panel. Imputation of BRASS and EIRA was previously reported [28,33], and we followed the same imputation procedures for the remaining datasets. Imputation yielded posterior genotype probabilities as well as imputation quality scores at SNPs not genotyped with a minor allele frequency $\geq 1\%$ in HapMap CEU. We removed imputed SNPs with imputation 'info' scores <0.5 or MAF $<1\%$ in any of the datasets.

Expression profile and eQTL data

Gene expression levels were quantified using mRNA derived from peripheral blood mononuclear cells (PBMCs) using Affymetrix Human Genome U133 Plus 2.0, for 255 multiple sclerosis patients in the Comprehensive Longitudinal Investigation of MS at the Brigham and Women's Hospital [34], either untreated ($N = 83$) or treated with interferon-beta ($N = 105$) or glatiramer acetate ($N = 67$). The raw intensity values were subject to quality control based on the recommended pipeline available in the simpleaffy and affyPLM R Bioconductor packages, and were then normalized using GCRMA ($N = 228$). The data are available on the Gene Expression Omnibus website (GSE16214). Expression levels for 17,390 probes mapping to 9,665 Ensembl transcripts were adjusted for confounding factors including age, gender, drug and batch using principle components and Bayesian factor analysis [35], and used in eQTL association analyses. Genotype data were collected on the Affymetrix 550K GeneChip 6.0 platform as a part of a previously published study [36]. Allelic dosages from imputed data (HapMap Phase II CEU samples; >2 million SNPs, MACH imputation quality >0.1 and $\text{MAF}>=0.05$) were used for association analysis. *Cis*-eQTLs were identified $+/-1$ Mb of transcription start sites (TSS) in the *1q23* locus region. Significance was evaluated by 10,000 permutations per gene, and false discovery rates were calculated based on cis-eQTL analyses in the total of 9,665 genes [37].

Additional expression profile data were available for subsets of samples that were part of two cohorts in our GWAS. Expression data from patients enrolled in the BRASS registry have been previously published [38]. Expression data were collected on Affymetrix Gene Chip U133 Plus 2 microarrays. BRASS patients had either cross-sectional expression data ($n = 132$, assayed at the time the patient was enrolled in BRASS) or pre- and post-treatment expression data ($n = 17$ samples, 8 treated with etanercept). Of these, $n = 87$ patients had expression and GWAS data. For patients with pre- and post-treatment data, we used the "baseline" pre-treatment expression data for cross-sectional analysis. In ABCoN, 65 RA patients ($n = 23$ treated with etanercept) had both pre- and post-treatment expression data, as well as ΔDAS clinical data [39], and $n = 45$ patients had expression and GWAS data. As with BRASS, we use the "baseline" pre-treatment expression data for cross-sectional analysis. For ABCoN expression profile data were collected on Illumina Human WG6v3 microarrays and were quantile normalized according to Illumina recommended protocols. Within both BRASS and ABCoN, expression data were normalized to the mean and standard deviation within each collection. For prospective analyses of expression data and ΔDAS, we combined BRASS and ABCoN to include 31 etanercept-treated patients and 78 anti-TNF-treated patients.

Statistical analyses

In our primary GWAS analysis, we tested each SNP for association with ΔDAS using linear regression adjusted for baseline DAS and the first 3 PCA eigenvectors in each collection. In our secondary GWAS analysis, we modeled SNPs predicting EULAR good response *versus* EULAR non-response using logistic regression, again adjusting for start-DAS value and the first three eigenvectors. Association analysis was done using SNPTEST [32] assuming an additive genetic model. Genomic control λ_{GC} values [40] for genotyped SNPs only and all SNPs were calculated, and no inflation or deflation was observed in the distributions of association test results. We then conducted inverse variance-weighted meta-analysis to combine results across the four datasets, and conducted Cochran's Q tests for heterogeneity using the β coefficients [41]. We further divided samples into 3 subsets according to drug (etanercept, infliximab or adalimumab). GWAS analysis for each group followed the same analysis procedure. Meta-analysis and heterogeneity tests were conducted using SAS. Expression analyses utilized linear regression or Spearman rank correlation, also using SAS. We tested for effects of cohort, age, gender and concurrent methotrexate, and results are shown using significant covariates as indicated.

Supporting Information

Figure S1 Quantile–quantile (QQ) plots for ΔDAS and response analysis, with genomic control λ_{GC} values.
(TIF)

Figure S2 GWAS results for the good response versus non-response phenotype. Shown are strengths of association ($-$Log10 P-value) for each SNP versus position along chromosomes 1 to 22. A) All samples ($n = 1{,}708$). B) Etanercept-treated patients ($n = 472$). C) Infliximab-treated patients ($n = 599$). D) Adalimumab-treated patients ($n = 636$).
(TIF)

Figure S3 Forest plot of replication results for the CD84 SNP rs6427528, in patients treated with anti-TNF drugs other than etanercept (infliximab & adalimumab).
(TIF)

Figure S4 Forest plot of CD84 result in patients treated with etanercept, subset by all collections.
(TIF)

Figure S5 Patterns of linkage disequilibrium (LD) at the CD84 locus in HapMap. Shown patterns of LD for CEU (top panel) and CHBJPT (bottom panel).
(TIF)

Table S1 Sample information for each of thirteen clinical batches.
(DOC)

Table S2 Clinical multivariate model for the ΔDAS phenotype.
(DOC)

Table S3 GWAS results for all SNPs achieving $P<10^{-6}$ from any analysis.
(XLS)

Table S4 Sample and clinical data summary for replication samples.
(DOC)

Acknowledgments

We thank Lars Klareskog and Lars Alfredsson for their contribution to the EIRA cohort, and the Swedish Rheumatology Register and Biologics Register (ARTIS) for providing follow-up data for the patients in the EIRA and KI study groups. We thank participants in the Biologics in Rheumatoid Arthritis Genetics and Genomics Study Syndicate (BRAGGSS).

Author Contributions

Conceived and designed the experiments: JC EAS RMP. Performed the experiments: JC EAS RMP. Analyzed the data: JC EAS RMP. Contributed reagents/materials/analysis tools: SS CM DD GT TR MUM HC KI CT YO SW JA HY SM AT KO FM TM NG MK AWM JDI AGW KLH MH MED P-PT JBAC IEvdH-B GJW PLCMvR MvdL H-JG NAS CFA TWJH REMT RPK SLB LAC LWM JEF NdV BES PLDJ SR MEW PKG XM AB LP MJHC EWK. Wrote the paper: JC EAS RMP. All authors reviewed and approved the manuscript.

References

1. Klareskog L, Catrina AI, Paget S (2009) Rheumatoid arthritis. Lancet 373: 659–672.
2. Scott DL, Wolfe F, Huizinga TW (2010) Rheumatoid arthritis. Lancet 376: 1094–1108.
3. McInnes IB, Schett G (2011) The pathogenesis of rheumatoid arthritis. N Engl J Med 365: 2205–2219.
4. Aeberli D, Seitz M, Juni P, Villiger PM (2005) Increase of peripheral CXCR3 positive T lymphocytes upon treatment of RA patients with TNF-alpha inhibitors. Rheumatology (Oxford) 44: 172–175.
5. Agnholt J, Dahlerup JF, Kaltoft K (2003) The effect of etanercept and infliximab on the production of tumour necrosis factor alpha, interferon-gamma and GM-CSF in in vivo activated intestinal T lymphocyte cultures. Cytokine 23: 76–85.
6. Catrina AI, Trollmo C, af Klint E, Engstrom M, Lampa J, et al. (2005) Evidence that anti-tumor necrosis factor therapy with both etanercept and infliximab induces apoptosis in macrophages, but not lymphocytes, in rheumatoid arthritis joints: extended report. Arthritis Rheum 52: 61–72.
7. Scallon BJ, Moore MA, Trinh H, Knight DM, Ghrayeb J (1995) Chimeric anti-TNF-alpha monoclonal antibody cA2 binds recombinant transmembrane TNF-alpha and activates immune effector functions. Cytokine 7: 251–259.
8. Gudbrandsdottir S, Larsen R, Sorensen LK, Nielsen S, Hansen MB, et al. (2004) TNF and LT binding capacities in the plasma of arthritis patients: effect of etanercept treatment in juvenile idiopathic arthritis. Clin Exp Rheumatol 22: 118–124.
9. Plant D, Prajapati R, Hyrich KL, Morgan AW, Wilson AG, et al. (2012) Replication of association of the PTPRC gene with response to anti-tumor necrosis factor therapy in a large UK cohort. Arthritis Rheum 64: 665–670.
10. Prajapati R, Plant D, Barton A (2011) Genetic and genomic predictors of anti-TNF response. Pharmacogenomics 12: 1571–1585.
11. Cui J, Saevarsdottir S, Thomson B, Padyukov L, van der Helm-Van Mil AH, et al. (2010) Rheumatoid arthritis risk allele PTPRC is also associated with response to anti-tumor necrosis factor alpha therapy. Arthritis Rheum 62: 1849–1861.
12. Plant D, Bowes J, Potter C, Hyrich KL, Morgan AW, et al. (2011) Genome-wide association study of genetic predictors of anti-tumor necrosis factor treatment efficacy in rheumatoid arthritis identifies associations with polymorphisms at seven loci. Arthritis Rheum 63: 645–653.
13. Liu C, Batliwalla F, Li W, Lee A, Roubenoff R, et al. (2008) Genome-wide association scan identifies candidate polymorphisms associated with differential response to anti-TNF treatment in rheumatoid arthritis. Mol Med 14: 575–581.
14. Prevoo ML, van 't Hof MA, Kuper HH, van Leeuwen MA, van de Putte LB, et al. (1995) Modified disease activity scores that include twenty-eight-joint counts. Development and validation in a prospective longitudinal study of patients with rheumatoid arthritis. Arthritis Rheum 38: 44–48.
15. van Gestel AM, Prevoo ML, van 't Hof MA, van Rijswijk MH, van de Putte LB, et al. (1996) Development and validation of the European League Against Rheumatism response criteria for rheumatoid arthritis. Comparison with the preliminary American College of Rheumatology and the World Health Organization/International League Against Rheumatism Criteria. Arthritis Rheum 39: 34–40.
16. Ward LD, Kellis M (2012) HaploReg: a resource for exploring chromatin states, conservation, and regulatory motif alterations within sets of genetically linked variants. Nucleic Acids Res 40: D930–934.
17. Ernst J, Kheradpour P, Mikkelsen TS, Shoresh N, Ward LD, et al. (2011) Mapping and analysis of chromatin state dynamics in nine human cell types. Nature 473: 43–49.
18. Cooper GM, Stone EA, Asimenos G, Green ED, Batzoglou S, et al. (2005) Distribution and intensity of constraint in mammalian genomic sequence. Genome Res 15: 901–913.
19. Soliman MM, Hyrich KL, Lunt M, Watson KD, Symmons DP, et al. (2012) Rituximab or a second anti-TNF therapy for rheumatoid arthritis patients who have failed their first anti-TNF? Comparative analysis from the British Society for Rheumatology Biologics Register. Arthritis Care Res (Hoboken).
20. Tangye SG, Nichols KE, Hare NJ, van de Weerdt BC (2003) Functional requirements for interactions between CD84 and Src homology 2 domain-containing proteins and their contribution to human T cell activation. J Immunol 171: 2485–2495.
21. Martin M, Romero X, de la Fuente MA, Tovar V, Zapater N, et al. (2001) CD84 functions as a homophilic adhesion molecule and enhances IFN-gamma secretion: adhesion is mediated by Ig-like domain 1. J Immunol 167: 3668–3676.
22. Padyukov L, Lampa J, Heimburger M, Ernestam S, Cederholm T, et al. (2003) Genetic markers for the efficacy of tumour necrosis factor blocking therapy in rheumatoid arthritis. Ann Rheum Dis 62: 526–529.
23. Coenen MJ, Enevold C, Barrera P, Schijvenaars MM, Toonen EJ, et al. (2010) Genetic variants in toll-like receptors are not associated with rheumatoid arthritis susceptibility or anti-tumour necrosis factor treatment outcome. PLoS ONE 5: e14326. doi:10.1371/journal.pone.0014326
24. Toonen EJ, Coenen MJ, Kievit W, Fransen J, Eijsbouts AM, et al. (2008) The tumour necrosis factor receptor superfamily member 1b 676T>G polymorphism in relation to response to infliximab and adalimumab treatment and disease severity in rheumatoid arthritis. Ann Rheum Dis 67: 1174–1177.
25. Miceli-Richard C, Comets E, Verstuyft C, Tamouza R, Loiseau P, et al. (2008) A single tumour necrosis factor haplotype influences the response to adalimumab in rheumatoid arthritis. Ann Rheum Dis 67: 478–484.
26. Canhao H, Faustino A, Martins F, Fonseca JE (2011) Reuma.pt - the rheumatic diseases portuguese register. Acta Reumatol Port 36: 45–56.
27. Okada Y, Terao C, Ikari K, Kochi Y, Ohmura K, et al. (2012) Meta-analysis identifies nine new loci associated with rheumatoid arthritis in the Japanese population. Nat Genet.
28. Stahl EA, Raychaudhuri S, Remmers EF, Xie G, Eyre S, et al. (2010) Genome-wide association study meta-analysis identifies seven new rheumatoid arthritis risk loci. Nat Genet 42: 508–514.
29. Plenge RM, Seielstad M, Padyukov L, Lee AT, Remmers EF, et al. (2007) TRAF1-C5 as a Risk Locus for Rheumatoid Arthritis – A Genomewide Study. N Engl J Med 357: 1199–1209.
30. Purcell S, Neale B, Todd-Brown K, Thomas L, Ferreira MA, et al. (2007) PLINK: a tool set for whole-genome association and population-based linkage analyses. Am J Hum Genet 81: 559–575.
31. Price AL, Patterson NJ, Plenge RM, Weinblatt ME, Shadick NA, et al. (2006) Principal components analysis corrects for stratification in genome-wide association studies. Nat Genet 38: 904–909.
32. Marchini J, Howie B, Myers S, McVean G, Donnelly P (2007) A new multipoint method for genome-wide association studies by imputation of genotypes. Nat Genet 39: 906–913.
33. Stahl EA, Wegmann D, Trynka G, Gutierrez-Achury J, Do R, et al. (2012) Bayesian inference analyses of the polygenic architecture of rheumatoid arthritis. Nat Genet.
34. Gauthier SA, Glanz BI, Mandel M, Weiner HL (2006) A model for the comprehensive investigation of a chronic autoimmune disease: the multiple sclerosis CLIMB study. Autoimmun Rev 5: 532–536.
35. Stegle O, Parts L, Durbin R, Winn J (2010) A Bayesian framework to account for complex non-genetic factors in gene expression levels greatly increases power in eQTL studies. PLoS Comput Biol 6: e1000770. doi:10.1371/journal.pcbi.1000770
36. De Jager PL, Jia X, Wang J, de Bakker PI, Ottoboni L, et al. (2009) Meta-analysis of genome scans and replication identify CD6, IRF8 and TNFRSF1A as new multiple sclerosis susceptibility loci. Nat Genet 41: 776–782.
37. Stranger BE, Nica AC, Forrest MS, Dimas A, Bird CP, et al. (2007) Population genomics of human gene expression. Nat Genet 39: 1217–1224.
38. Parker A, Izmailova ES, Narang J, Badola S, Le T, et al. (2007) Peripheral Blood Expression of Nuclear Factor-kappaB-Regulated Genes Is Associated with Rheumatoid Arthritis Disease Activity and Responds Differentially to Anti-Tumor Necrosis Factor-alpha versus Methotrexate. J Rheumatol 34: 1817–1822.
39. Batliwalla FM, Baechler EC, Xiao X, Li W, Balasubramanian S, et al. (2005) Peripheral blood gene expression profiling in rheumatoid arthritis. Genes Immun 6: 388–397.
40. Devlin B, Roeder K, Wasserman L (2001) Genomic control, a new approach to genetic-based association studies. Theor Popul Biol 60: 155–166.
41. de Bakker PI, Ferreira MA, Jia X, Neale BM, Raychaudhuri S, et al. (2008) Practical aspects of imputation-driven meta-analysis of genome-wide association studies. Hum Mol Genet 17: R122–128.

JOURNAL OF COMPUTATIONAL BIOLOGY
Volume 19, Number 1, 2012
© Mary Ann Liebert, Inc.
Pp. 55–67
DOI: 10.1089/cmb.2010.0227

Population Model–Based Inter-Diplotype Similarity Measure for Accurate Diplotype Clustering

RITSUKO ONUKI,[1] RYO YAMADA,[2] RUI YAMAGUCHI,[3]
MINORU KANEHISA,[1] and TETSUO SHIBUYA[3]

ABSTRACT

Classification of the individuals' genotype data is important in various kinds of biomedical research. There are many sophisticated clustering algorithms, but most of them require some appropriate similarity measure between objects to be clustered. Hence, accurate inter-diplotype similarity measures are always required for classification of diplotypes. In this article, we propose a new accurate inter-diplotype similarity measure that we call the population model-based distance (PMD), so that we can cluster individuals with diplotype SNPs data (i.e., unphased-diplotypes) with higher accuracies. For unphased-diplotypes, the allele sharing distance (ASD) has been the standard to measure the genetic distance between the diplotypes of individuals. To achieve higher clustering accuracies, our new measure PMD makes good use of a given appropriate population model which has never been utilized in the ASD. As the population model, we propose to use an hidden Markov model (HMM)-based model. We call the PMD based on the model the HHD (HIT HMM–based Distance). We demonstrate the impact of the HHD on the diplotype classification through comprehensive large-scale experiments over the genome-wide 8930 data sets derived from the HapMap SNPs database. The experiments revealed that the HHD enables significantly more accurate clustering than the ASD.

Key words: algorithms, statistics, strings, suffix trees.

1. INTRODUCTION

Single nucleotide polymorphisms (SNPs) are the most fundamental genetic polymorphisms in human genomes (Kim and Misra, 2007), and classification of individuals with the individual SNPs data is very useful in various kinds of biomedical research, especially in population genetics and genetic epidemiology (Conrad et al., 2006; Jakobsson et al., 2008). Accurate classification of individual SNPs data will help study of genotype variations, especially when different genotypes prevail in different populations or subgroups.

There are various sophisticated clustering methods for general data (not limited for clustering SNPs data), many of which (e.g., Ward's method [Team RDC, 2007; Ward, 1963; Ward and Hook, 1963],

[1]Bioinformatics Center, Institute for Chemical Research, Kyoto University, Kyoto Japan.
[2]Center for Genomic Medicine, Graduate School of Medicine, Kyoto University, Kyoto, Japan.
[3]Human Genome Center, Institute of Medical Science, University of Tokyo, Tokyo, Japan.

k-Medoid [Kaufman and Rousseuw, 1990], DBSCAN [Ester et al., 1996], and most of the phylogenetic clustering algorithms such as the famous neighbor joining method [Saitou and Nei, 1987]) require appropriate similarity measures between target objects. Designing accurate similarity measure for the objects to be clustered is essential for these similarity-based clustering algorithms.

For SNPs data, there have been proposed various clustering algorithms for clustering haplotypes (i.e., haplotype-alleles, not diplotypes),[1] and various types of similarity measures have been proposed for haplotype data (Jin et al., 2010; Li and Jiang, 2005; Li et al., 2006).[2] But the human genome is diallelic, and in many cases we observe only the unordered (i.e., unphased) pair of alleles at each locus, instead of ordered (i.e., phased) allele data, due to the high costs required for deciphering unphased allele data to accurate phased ones. In this article, we call a phased pair of haplotypes a ''haplotype-diplotype,'' and we call an unphased pair of haplotypes a ''unphased-diplotype.''

Much work has been done on clustering the unphased-diplotype data. They can be categorized into two types: distance-based methods (Bowcock et al., 1994; Gao and Starmer, 2007) and statistics-based methods (Falush et al., 2003; Pritchard et al., 2000). The distance-based methods utilize a distance measure between two objects, while statistics-based methods are based on the statistical behavior of objects. In this article, we focus on the distance-based clustering methods for unphased-diplotype data. Most previous distance-based methods utilize a similarity measure called the allele sharing distance (ASD) (Gao and Martin, 2009; Jakobsson et al., 2008; Mao et al., 2007; Witherspoon et al., 2007) (see Section 2.1.1). The ASD is a simple and straightforward extension of the Hamming distance, and is the most standard and frequently used similarity measure between a pair of unphased-diplotypes.

In genetic analysis, it is very important to consider properties of populations that are different among genetically distinct populations (Beaty et al., 2005; Fallin et al., 2001; Witherspoon et al., 2007). It should also be true with designing similarity measures for unphased-diplotypes. But the measure ASD does not utilize any population information in obtaining the similarity values. Thus, in this article, we will first propose a new similarity measure called the population model-based distance (PMD) for unphased-diplotypes, which incorporates the population information from an appropriate population model. As the model, we will propose to use an hidden Markov model (HMM)–based model predicted by a standard HMM-based phasing software called HIT (Rastas et al., 2005). We call the PMD based on the model the HHD (the HIT HMM-based distance). We will show the superiority of our new measure HHD over the previous standard ASD through comprehensive experiments over the genome-wide HapMap data (International HapMap Consortium, 2005).

The organization of this article is as follows. In Section 2, we describe previous work on which our method is based. In Section 3, we describe our new measure. In Section 4, we compare the ASD and the HHD through comprehensive experiments over large-scale HapMap data sets to evaluate the impact of the HHD. In Section 5, we conclude.

1.1. Notations and definitions

We assume all SNPs are diallelic. We consider n diplotypes over m SNP loci from the same chromosome. These loci are numbered $1, 2, \cdots, m$ in the physical order. A SNP-allele for a SNP locus is an element in set $\mathcal{S} = \{1, 0\}$ where 1 and 0 denote the major and minor SNP-alleles, respectively. A haplotype-allele is a sequence of SNP-alleles and is represented by a sequence in $\mathcal{S}^m$ (e.g., $10101 \in \mathcal{S}^5$). A SNP-diplotype for a SNP locus is an unordered pair of SNP-allele in $\mathcal{D} = \mathcal{S} \times \mathcal{S}$(e.g., $\{0, 1\} \in \mathcal{D}$). An unphased-diplotype is a sequence of SNP-diplotype and is represented by a sequence in $\mathcal{D}^m$(e.g., $\{1, 0\} - \{0, 0\} - \{1, 0\} - \{1, 1\} - \{1, 0\} \in \mathcal{D}^5$). Given unphased-diplotypes, the phasing problem is to find the most probable corresponding haplotype-allele pairs that could have generated the unphased-diplotypes. A phased haplotype-allele pair is called a haplotype-diplotype (e.g., {10010, 00111}).

[1] There are also many algorithms proposed for clustering SNP loci (Yang and Tabus, 2007), instead of individuals, but we do not deal with these problems in this article.

[2] Various inter-population distances have also been proposed (Cornuet et al., 1999), but we will not deal with these in this article.

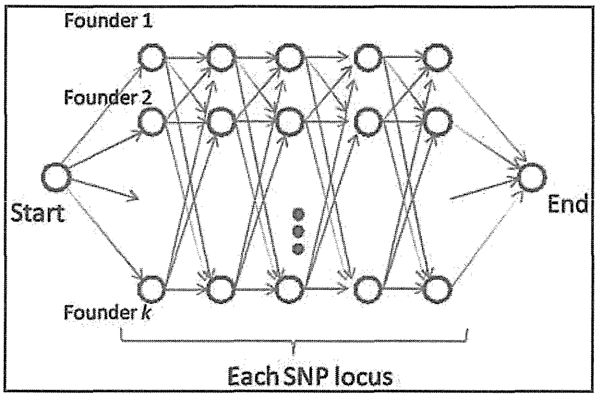

FIG. 1. The HMM model of the HIT. In the HMM, a set of nodes in a row corresponds to states of one founder (i.e., ancestor) haplotype-allele. A set of nodes in a column corresponds to states of one locus. Each node (except for the start and end nodes) emits 1 or 0 with some estimated probabilities, which correspond to the major and minor alleles respectively. A path from the start node to the end node corresponds to a haplotype-allele. The HMM emits a haplotype-diplotype as an unordered pair of two paths from the start node to the end node, randomly based on the probabilities estimated for edges. The observers can only see the unphased-diplotype that corresponds to the emitted haplotype-diplotype.

2. PREVIOUS WORK

In this section, we describe previous work on which our work is based. In Section 2.1, we describe the definitions of measures in previous work (e.g., the ASD). In Section 2.2, we describe the HIT algorithm on which our new distance measure is based. In Section 2.3, we describe a clustering algorithm and an evaluation method for clustering that we will use in the experiments in Section 4.

2.1. Previous measures for inter-individual genetic distances

2.1.1. Allele sharing distance. The most standard inter-diplotype distance is the ASD (Gao and Martin, 2009; Jakobsson et al., 2008; Mao et al., 2007; Witherspoon et al., 2007), defined as follows. For two unphased-diplotypes $\mathbf{g}$, $\mathbf{g}' \in \mathcal{D}^m$ (i.e., m is the number of SNP loci), the ASD between the diplotypes $\mathbf{g}$ and $\mathbf{g}'$ is defined as follows:

$$D(\mathbf{g}, \mathbf{g}') = \frac{1}{2m}\sum_{\ell=1}^{m} d(\mathbf{g}[\ell], \mathbf{g}'[\ell]), \tag{1}$$

where $\mathbf{g}[\ell]$ denotes the ℓ-th SNP-diplotype of unphased-diplotype $\mathbf{g}$, and $d(\mathbf{g}[\ell], \mathbf{g}'[\ell])$ is the number of SNP-alleles which are not shared between $\mathbf{g}$ and $\mathbf{g}'$ at the ℓ-th locus.

2.1.2. Haplotype similarity measure. The most common and simplest measurement for the similarity between DNA sequences, including the haplotype-allele data, is the hamming distance (Cover and Thomas, 1991; Isaev, 2004; Lesk, 2005; Li and Jiang, 2005; Tzeng et al., 2003). For a haplotype-allele $\mathbf{h} \in \mathcal{S}^m$ (where m is the length of $\mathbf{h}$), let $\mathbf{h}[k]$ denote the SNP-allele at the k-th locus of $\mathbf{h}$. The hamming distance between two haplotype-alleles $\mathbf{h}$ and $\mathbf{h}'$ is defined as

$$s(h, h') = \sum_{k=1}^{m} I(\mathbf{h}[k], \mathbf{h}'[k]), \tag{2}$$

where $I(a, b) = 0$ if $a = b$ and $I(a, b) = 1$ otherwise. As the hamming distance is length-dependent, we define the following $A(\mathbf{h}, \mathbf{h}')$ as a length-independent distance between haplotype-alleles $\mathbf{h}$ and $\mathbf{h}'$:

$$A(\mathbf{h}, \mathbf{h}') = \frac{s(\mathbf{h}, \mathbf{h}')}{m}. \tag{3}$$

2.2. HIT algorithm

The Haplotype Inference Technique (HIT) algorithm (Rastas et al., 2005) is an HMM-based algorithm for phasing unphased-diplotypes. The algorithm utilizes the HMM (Rabiner and Juang, 1986). The HMM of the HIT is designed to simulate multiple set of ancestors (i.e., founders).[3] The HMM is trained from a set

[3] According to Rastas et al. (2005), the optimal number of ancestors is around 7 for most cases. Thus, we also use the HMM model with 7 ancestors in the experiments in Section 4.

of unphased-diplotypes in an unsupervised way with the EM algorithm (Durbin et al., 1998). Figure 1 shows the HMM model used in the HIT. The HIT algorithm phases an unphased haplotype-diplotype by heuristically finding the haplotype-diplotype with the highest emission probability from the HMM.

2.3. *Clustering methods*

In this section, we describe the clustering method and the method for evaluating the results, which we will use in Section 4.

2.3.1. Ward's method. We use Ward's minimum variance algorithm (Team RDC, 2007; Ward, 1963; Ward and Hook, 1963), which is a widely used hierarchical clustering method, to infer clusters based on the ASD or the HHD in Section 4.[4] Given n items $I_1, I_2, \cdots, I_n$, a distance matrix $\{w_{ij}\}$ where w_{ij} denotes the distance between I_i and I_j, and some fixed positive integer k ($k < n$), the Ward's method clusters the n items into k clusters by the following $n - k - 1$ steps.[5] At first the algorithm considers n clusters each of which contains only 1 item, i.e., $\mathcal{C}_1 = \{\{I_1\}, \{I_2\}, \cdots, \{I_n\}\}$. Then the algorithm reduces the number of clusters one by one in each step as follows. In the m-th step of the algorithm, two clusters are merged into a cluster to minimize $\sum_{C \in \mathcal{C}_{m+1}} \sum_{I_i, I_j \in C} w_{ij}^2/|C|$, where $\mathcal{C}_i$ denotes the set of clusters before the i-th step of the algorithm. This bottom-up approach is repeated until $|\mathcal{C}_m| = k$.

2.3.2. How to evaluate the clustering results. To evaluate the clustering results, we use the classification error rate (CER) (Gao and Starmer, 2007). The CER is the rate of elements that are assigned to incorrect clusters in clustering results. To know the assignment is correct or not, we need to know the labels of each cluster, but Ward's algorithm does not assign any labels onto the output clusters. In the experiment, we use the minimum CER among all the possible assignments of the population labels, to evaluate the clustering results.

3. NEW UNPHASED-DIPLOTYPE DISTANCE MEASURES

In this section, we first propose in Section 3.1 a new measure for the distance between two unphased-diplotypes, the PMD. The PMD is a general concept of distance measures, and we will give an example of the PMD which we call the HHD in Section 3.2. In Section 3.3, we discuss the properties of the proposed measures.

3.1. *Population model–based distance*

Before defining our new measure called the PMD, we first extend the haplotype similarity measure described in Section 2.1.2 so that we can deal with the distances between two haplotype-diplotypes instead of haplotype-alleles, as follows. Let $a = \{\mathbb{h}_1, \mathbb{h}_2\}$ and $a' = \{\mathbb{h}'_1, \mathbb{h}'_2\}$ be haplotype-diplotypes to be compared, where $\mathbb{h}_1, \mathbb{h}_2, \mathbb{h}'_1, \mathbb{h}'_2 \in \mathcal{S}^m$. We define the distance between haplotype-diplotypes a and a' as

$$H(a, a') = \min\left\{\frac{A(\mathbb{h}_1, \mathbb{h}'_1) + A(\mathbb{h}_2, \mathbb{h}'_2)}{2}, \frac{A(\mathbb{h}_1, \mathbb{h}'_2) + A(\mathbb{h}_2, \mathbb{h}'_1)}{2}\right\}, \tag{4}$$

where A is the haplotype similarity measure defined in Section 2.1.2. But we cannot compute this value for unphased-diplotypes, as we cannot know the actual haplotype-diplotypes. To enable it, we extend the above haplotype-diplotype distance H for unphased-diplotypes by utilizing some given population model $\mathcal{M}$ as follows.

For any unphased-diplotype, we can enumerate corresponding haplotype-diplotype candidates.[6] For example, there are four haplotype-diplotype candidates for unphased-diplotype $\{1, 0\} - \{1, 0\} - \{1, 0\}$, i.e., $\{111, 000\}$, $\{110, 001\}$, $\{101, 010\}$, and $\{011, 011\}$. For unphased-diplotypes $\mathbf{g}$, $\mathbf{g}' \in \mathcal{D}^m$, let $c_i = \{\mathbb{h}_{i1}, \mathbb{h}_{i2}\}$ $(1 \leq i \leq M)$ and $c'_j = \{\mathbb{h}'_{\mathrm{j}1}, \mathbb{h}'_{\mathrm{j}2}\}$ $(1 \leq j \leq M')$ be the i-th and the j-th candidate haplotype-diplotypes for

[4] We used the statistical software, R, to implement this algorithm.
[5] The ASD or the HHD values will be used as w_{ij} in Section 4.
[6] *Phasing* is the process of finding the most probable haplotype-diplotype, utilizing some population information.

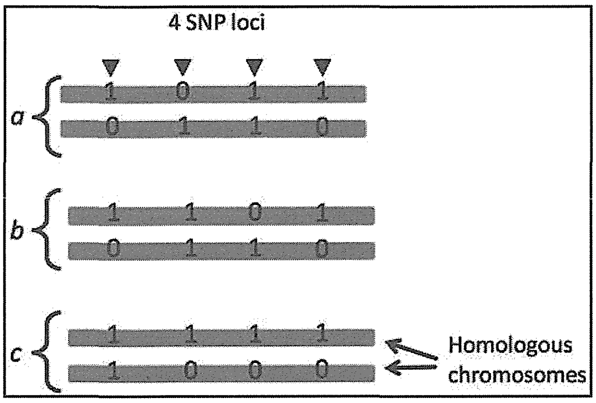

FIG. 2. Haplotype-diplotype examples on which we can observe difference between the ASD and the PMD.

g and g′, respectively. M and M' are the numbers of haplotype-diplotype candidates for g and g′, respectively.

If we were given a population model $\mathcal{M}$, we can compute the probability $Prob(c|\mathbf{g}, \mathcal{M})$ that a haplotype-diplotype candidate c is correct for the unphased-diplotype data g. Let $p_i = Prob(c_i|\mathbf{g}, \mathcal{M})$ and $p'_j = Prob(c'_j|\mathbf{g}', \mathcal{M})$ be the conditional probabilities of the candidate haplotype-diplotypes c_i and c'_j under the model $\mathcal{M}$. Then the $PMD_{\mathcal{M}}$ between two haplotype-diplotypes g and g′ is defined as follows:

$$PMD_{\mathcal{M}}(\mathbf{g}, \mathbf{g}') = \sum_{i=1}^{M} \sum_{j=1}^{M'} H(c_i, c'_j) \cdot q_i \cdot q'_j, \tag{5}$$

where $q_i = p_i / (\sum_{k=1}^{M} p_k)$ and $q'_j = p'_j / (\sum_{k=1}^{M'} p'_k)$. q_i and q'_j are the normalized predicted conditional probabilities of the candidate haplotype-diplotypes c_i and c'_j, respectively.[7] Note that the PMD is the expected value of the distance between candidate haplotype-diplotypes, $H(c_i, c'_j)$, under the population model$\mathcal{M}$.

3.2. HIT HMM-based Distance

To compute the PMD in Section 3.1, we need an appropriate model for the population. In the following, we propose an example of the PMD that we call the HHD.[8] To define the HHD, we propose to use the HMM model used in the HIT algorithm (Rastas et al., 2005) (described in Section 2.2) as the population model for the PMD as follows.

The HMM defined in the HIT algorithm can be considered as a predicted population model. Thus, we first train the HMM from all the unphased-diplotype data that are in our hand, and then we define the HHD as follows. Let $\mathcal{M}^*$ denote the HMM model obtained with the HIT. Then we define the HHD as

$$HHD(\mathbf{g}, \mathbf{g}') = PMD_{\mathcal{M}^*}(\mathbf{g}, \mathbf{g}'). \tag{6}$$

Note that the probability of each haplotype-diplotype candidate is computed as the conditional emission probability of the candidate from the HMM, which can be computed by the forward algorithm (Durbin et al., 1998) for the HMM.

3.3. Discussions on the PMD

3.3.1. The PMD and the multiple founder hypothesis. In many regions (especially in important regions) of the human genome, the haplotype-alleles of the majority in populations can be categorized into a small number of types (Bhatia et al., 2010; Cirulli and Goldstein, 2010), which suggest that only a small number of founder (or ancestral) haplotype-alleles spread over the population on those regions. This

[7] Note that $\sum_{k=1}^{M} p_k = \sum_{k=1}^{M} p'_k = 1$ and there is no need to normalize the probabilities if we enumerate all the candidates. But we need to normalize them in case we ignore the candidates with very small probabilities. When we compute the HHD (which will be introduced in Section 3.2), we ignore candidates with very small probabilities.

[8] We also introduce other simpler examples of the PMD in Section 3.3.1.

Table 1. Distances between the Individuals in Figure 2

	(1) ASD				(2) $H = PMD_{\mathcal{M}_1}$				(3) $PMD_{\mathcal{M}_2}$		
	a	*b*	*c*		*a*	*b*	*c*		*a*	*b*	*c*
a	0	0.25	0.25	*a*	0	0.25	0.5	*a*	0	0.301	0.450
b	—	0	0.25	*b*	—	0	0.5	*b*	—	0	0.500
c	—	—	0	*c*	—	—	0	*c*	—	—	0

hypothesis of the existence of (a few but) multiple founder haplotype-alleles is very important and effective for various kinds of research, for example, the design of the experiments of linkage disequilibrium mapping (Chung et al., 2008; Gonzalez et al., 1999; Haiman et al., 2003) and the evolutionary history analysis of populations (Ahmad et al., 2002; Gaudieri et al., 1997).

The PMD well reflects the existence of the founder haplotype-alleles. In the example given in Figure 2, there are three individuals with haplotype-diplotypes $a = \{1011, 0110\}$, $b = \{1101, 0110\}$, and $c = \{1111, 1000\}$, but we assume that we know only the unphased-haplotypes, i.e., $\{1, 0\} - \{1, 0\} - \{1, 1\} - \{1, 0\}$, $\{1, 0\} - \{1, 1\}$-$\{1, 0\} - \{1, 0\}$ and $\{1, 1\} - \{1, 0\} - \{1, 0\} - \{1, 0\}$, respectively. We can easily see that the ASD between any two of these three individuals is 0.25 (Table 1*(1)*), and therefore we cannot cluster these three individuals based on the ASD.

The distance between two sequences are often measured by the number of point mutations between them (i.e., we consider two sequences to be very distant to each other if there are many mutations between them). We can define the number of mutations under the assumption of existence of multiple founder haplotype-alleles (for details, see the Appendix). Table 2 shows the number under the assumption that there are two founder haplotype-alleles. According to the table, the clustering result of the three individuals should be the one in Figure 3, which cannot be obtained with the ASD. Note that the clustered individuals *a* and *b* share the same haplotype-allele, i.e., 0110, which also supports the validity of the clustering result.

Unlike the ASD, the haplotype-diplotype distance *H* reflects the numbers in Table 2 very well. The *H* value between individuals *a* and *b* is 0.25, which is the same value as the ASD, but *H* between *a* and *c* and *H* between *b* and *c* are 0.5 (Table 1*(2)*), which enable us to cluster the individuals as in Figure 3. It means the *H* values are more appropriate than the ASD values under the existence of the founder haplotype-alleles, at least in this case.

But we cannot compute the real *H* values unless we know the real haplotype-diplotypes. Instead, we can estimate them by computing the PMD if we are given some population model. Consider the two population models given in Table 3, where haplotype frequencies in the population are given.[9] Under the model $\mathcal{M}_1$, we can phase any of the three individuals' unphased-haplotypes correctly with 100% confidence, and the resulting $PMD_{\mathcal{M}_1}$ values are the same as the *H* values (Table 1*(2)*). But we cannot predict unphased-haplotypes with such high confidence in many cases, as in the case of the population model $\mathcal{M}_2$ where we have multiple haplotype-diplotype candidates for each unphased diplotype (see Table 4 and Table 1*(3)*).

If we cluster the three individuals based on the $H = PMD_{\mathcal{M}_1}$ values, we can obtain the same clusters as in Figure 3. Furthermore, we can still get the same clusters even if we use the $PMD_{\mathcal{M}_2}$ values instead. Thus, we assume that the PMD is more suitable than the ASD under the multiple founder hypothesis, if we are given an appropriate population model.

3.3.2. Influences of the linkage equilibrium. It is easy to imagine that the linkage equilibrium (LE) and the linkage disequilibrium (LD) should affect the similarity measures. In fact, the variance of the distribution of the ASD values among the individuals should converges to some value in $\Theta(1/m)$ where *m* is the number of the SNP loci in the region according to the central limit theorem, if the loci are independent to each other. It means that the variance of the ASD values should be smaller on the regions of LE. The PMD and its example HHD should also be influenced by the LE/LD. We compared the influences of the LE/LD to the ASD and the HHD by checking distances on the LE/LD regions obtained from the HapMap database (release 24) (International HapMap Consortium, 2005) as follows.

[9] The population models could be represented by many other methods. For example, we consider HMM-based models in Section 3.2.

TABLE 2. NUMBER OF MUATIONS BETWEEN EACH INDIVIDUAL UNDER THE ASSUMPTION THAT THERE ARE TWO FOUNDERS

	a	*b*	*c*
a	0	2	4
b	—	0	4
c	—	—	0

See Appendix how we obtain the number of mutaions for each pair of individuals.

We can determine whether a region is near to LE or to LD by counting the number of haplotype tagging SNPs (htSNPs) (Carlson et al., 2004; Johnson et al., 2001; Ke and Cardon, 2003; Meng et al., 2003; Rinaldo et al., 2005). The htSNPs are selected so that each SNP in the given region has a correlation larger than a threshold with at least one of the htSNPs. Thus, the regions with many htSNPs can be considered to be near the LE, and regions with few htSNPs can be considered to be near the LD.

We divided the set of SNPs in chromosome 1 into 658 blocks, each of which consists of 100 consecutive SNPs. For each block B, we counted the number h_B of htSNPs obtained by the software Tagger (de Bakker et al., 2005) with the default settings. We selected 100 blocks with the 100 smallest h_B values as the LD regions and also selected 100 blocks with the 100 largest h_B values as the LE regions.

For each of all these regions, we computed the ASD and the HHD measures among the 270 individuals in HapMap (which are the same as the 270 individuals used in Section 4), and computed the variances among the obtained $270 \times 269/2 = 36315$ distances of the ASD and of the HHD. Table 5 shows the difference between the variances of the ASD and the HHD measures. According to the P-values in the table, the HHD reflects the LD/LE effects more than the ASD.

4. APPLICATION TO HAPMAP DATA SETS

4.1. Data sets

In the experiments in Section 4.2, we will use the unphased-diplotype data sets of 22 autosomal chromosomes and X chromosome derived from HapMap release 24 (International HapMap Consortium, 2005). The data sets consist of unphased-diplotypes of 270 individuals: 90 Yoruba in Ibadan, Nigeria (YRI); 90 Utah residents with ancestry from northern and western Europe (CEU, from the CEPH diversity panel); and 90 Japanese in Tokyo, Japan, and Han Chinese in Beijing, China (CHB + JPT). There are 894,398 SNPs that are genotyped for all the above 270 individuals, which we used for our experiments. We divided the SNP set into 8,930 blocks, each of which consists of consecutive 100 SNPs, and we will perform comprehensive experiments against each of these blocks in Section 4.2.

4.2. Experimental results

In this section, we demonstrate the impact of incorporating the population information, by comparing the clustering accuracies by the ASD and that by the HHD on the HapMap data described in Section 4.1.

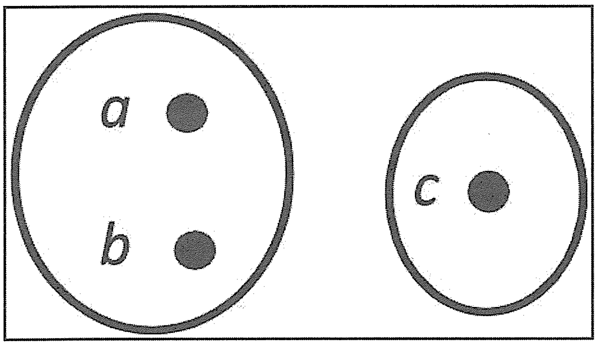

FIG. 3. Clustering results for individuals in Figure 2 based on the numbers of mutations (Table 2), $H = PMD_{\mathcal{M}_1}$ distances (Table 1*(2)*), or $PMD_{\mathcal{M}_2}$ distances (Table 1*(3)*). On the other hand, the ASD distances (Table 1*(1)*) cannot deduce this result.